Journal of Applied Physics

Room temperature semiconductor detectors for nuclear security

Cite as: J. Appl. Phys. **126**, 040902 (2019); https://doi.org/10.1063/1.5091805
Submitted: 05 February 2019 • Accepted: 01 June 2019 • Published Online: 30 July 2019

Paul M. Johns and Juan C. Nino

COLLECTIONS

This paper was selected as Featured

View Online Export Citation CrossMark

ARTICLES YOU MAY BE INTERESTED IN

Computational discovery of hard and superhard materials
Journal of Applied Physics **126**, 040901 (2019); https://doi.org/10.1063/1.5109782

Stable room-temperature thallium bromide semiconductor radiation detectors
APL Materials **5**, 106109 (2017); https://doi.org/10.1063/1.5001181

A perspective on topological nanophotonics: Current status and future challenges
Journal of Applied Physics **125**, 120901 (2019); https://doi.org/10.1063/1.5086433

Lock-in Amplifiers up to 600 MHz
Zurich Instruments
Watch

© 2019 Author(s).

Journal of Applied Physics PERSPECTIVE scitation.org/journal/jap

Room temperature semiconductor detectors for nuclear security

Cite as: J. Appl. Phys. **126**, 040902 (2019); doi: 10.1063/1.5091805
Submitted: 5 February 2019 · Accepted: 1 June 2019 ·
Published Online: 30 July 2019

View Online Export Citation CrossMark

Paul M. Johns[1,a)] and Juan C. Nino[2]

AFFILIATIONS

[1]Pacific Northwest National Laboratory, Detection Systems Group, Richland, Washington 99354, USA
[2]Department of Materials Science and Engineering, University of Florida, Gainesville, Florida 32601, USA

[a)]**Author to whom correspondence should be addressed:** paul.johns@pnnl.gov

ABSTRACT

Preventing radioactive sources from being used for harmful purposes is a global challenge. A requirement for solving the challenge is developing radiation detectors that are efficient, sensitive, and practical. Room temperature semiconductor detectors (RTSDs) are an important class of gamma-ray sensors because they can generate high-resolution gamma-ray spectra at ambient operating temperatures. A number of diverse and stringent requirements must be met for semiconducting materials to serve as sensors in RTSD spectrometers, which limits the number of candidates of interest that receive attention and undergo focused research and development efforts. Despite this, the development of new compounds for sensors in RTSDs is a thriving research field, and a number of materials with stunning potential as RTSD materials have emerged within the last decade. In this perspective, the state of the art in RTSD materials is examined, and emerging semiconducting compounds are reviewed. The highly developed CdTe, CdZnTe, HgI_2, and TlBr are first discussed to highlight the potential that can emerge from RTSD compounds in advanced stages of technological development. Thereafter, emerging compounds are reviewed by class from chalcogenides, iodides and chalcohalides, and organic-inorganic hybrid compounds. This work provides both a compilation of the physical and electronic properties of the emerging RTSD candidates and a perspective on the importance of material properties for the future of compounds that can transform the field of radiation detection science.

Published under license by AIP Publishing. https://doi.org/10.1063/1.5091805

I. INTRODUCTION

The average person has a very low risk of being unintentionally exposed to harmful amounts of non-naturally occurring radiation. However, because of the dangers presented from maliciously used nuclear materials, being able to detect radiation and radioactive sources used for harmful purposes is one of the primary global security concerns of the 21st century.[1,2] From the scope of international security, it is necessary to prevent rogue nations and terrorist groups from obtaining and deploying weapons of mass destruction made via radioactive materials. International treaties such as the 1968 Treaty on the Non-Proliferation of Nuclear Weapons (NPT) and the 1996 Comprehensive Test Ban Treaty (CTBT) rely on detection technology to discover the undeclared production of nuclear material, prevent trafficking, and analyze underground detonations. Likewise, one of the overarching goals of the United States' National Strategy for Counterterrorism has been to prevent terrorist development, acquisition, and use of weapons of mass destruction.[3] Doing so involves utilizing state-of-the-art technology to detect and interdict diverted nuclear materials.

There are a number of requirements that must be met for radiation sensors to be useful as instruments that detect the presence of radiation. The most basic criteria are as follows:

1. Be made of a material that efficiently absorbs gamma rays that pass through it.
2. Have the ability to produce a spectral response that enables the identification and characterization of radioactive sources.

Detectors that satisfy these two criteria can produce high signal-to-noise ratios upon gamma ray interactions, which enable the detection of radioactive sources. The better the combination of efficiency and signal resolution is in a gamma-ray detector, the faster that detector can detect and identify radiological threats. Additionally, for practical purposes, detector systems need to have reasonable sizes (on the order of several cubic centimeters for benchtop or

handheld applications); be thermally, mechanically, and electronically robust; and be produced at low cost.

A. Why are room temperature semiconductor detectors (RTSDs) important?

Most commercially available and deployed radiation detectors that provide a spectral response are based on either semiconductor or scintillation detection technology, with polyvinyltoluene (PVT), NaI:Tl, CsI:Tl, $LaBr_3$:Ce, $CeBr_3$, CsLiYCl:Ce (CLYC), $Bi_4Ge_3O_{12}$ (BGO), Si, Ge, and CdTe-based compounds serving as the most common sensor materials.[4] The most ubiquitous radiation detection material used in commercially produced radiation detection instruments is the scintillator NaI:Tl. Scintillators generate signals as the scintillation light produced in gamma-ray interactions is measured by a photodetector. While exhibiting poorer energy resolution than many alternate materials (around 7%–10% at 662 keV),[5] the use of advanced identification algorithms can allow systems with moderately sized NaI:Tl crystals to identify many isotopes down to gamma-ray fluxes between 1 and 0.1 γ/cm^2 s in a span of 1 or 2 min of measurement time.

The current industry performance benchmarks for detection systems are based on high purity Ge (HPGe) semiconductor sensors. Compared to a NaI:Tl crystal of a similar size, HPGe can detect and enable the identification of sources at an order of magnitude lower gamma-ray fluxes. The advantage of HPGe comes from the interaction mechanism by which semiconductor detectors generate signals from gamma rays. In a semiconductor, signals are produced directly from the ionized charges that are generated in interactions. A larger amount of information-carrying quanta are generated in this interaction mechanism that allows for energy resolution in photopeaks to be much better than scintillators. This, in turn, gives HPGe detectors greater signal-to-noise ratios that can then allow radioactive sources to be identified at farther standoff distances or shorter measurement times. For instance, a Ge-based detector cooled by liquid nitrogen can produce gamma-ray spectra with resolution below 0.8%.[6]

The drawback on HPGe detectors is that they need to be cooled to cryogenic temperatures in order to function optimally due to the intrinsically low room temperature value of the Ge bandgap (0.67 eV). At room temperature, thermal phonons excite electrons into the conduction band and can create too high of an electron density in the conduction band to distinguish signal from noise. Integrating cooling systems into a detector requires bulky sterling engines or cryogen reservoirs, which leads to increases in cost, weight, and power consumption requirements that reduce the practicality of the systems in field conditions.

Many semiconductors with larger bandgaps have come under investigation as candidate materials for radiation detectors that can identify and characterize sources at farther standoff distances and shorter measurement times than comparably sized NaI(Tl). These materials, RTSDs, can produce high-energy resolution spectral responses without the need for cooling. An RTSD detector presents the potential to serve as a crucial instrument in nuclear security applications that require the detection and identification of radioactive sources. Similar to HPGe, RTSDs are direct energy converters and function by converting energy from gamma rays into ionized charge carriers. A large number of quanta, in the form of electron/hole (e^-/h^+) pairs, are generated when gamma rays create ionization within semiconductors. This direct conversion process can provide excellent resolution in photopeaks within the resulting gamma-ray spectra. This can be clearly observed in Fig. 1 where a comparison of the spectra obtained from different scintillator and semiconductor sensors found in a range of commercially available spectrometers is presented.

II. PROPERTY CONSIDERATIONS FOR RTSDs

When designing a semiconductor to serve as a gamma-ray sensor, the key properties of consideration are density, atomic number, and the band gap of the compound. Because radiation stopping power is dictated by the effective atomic number and physical density of a material, it is logical to select the heaviest nonradioactive

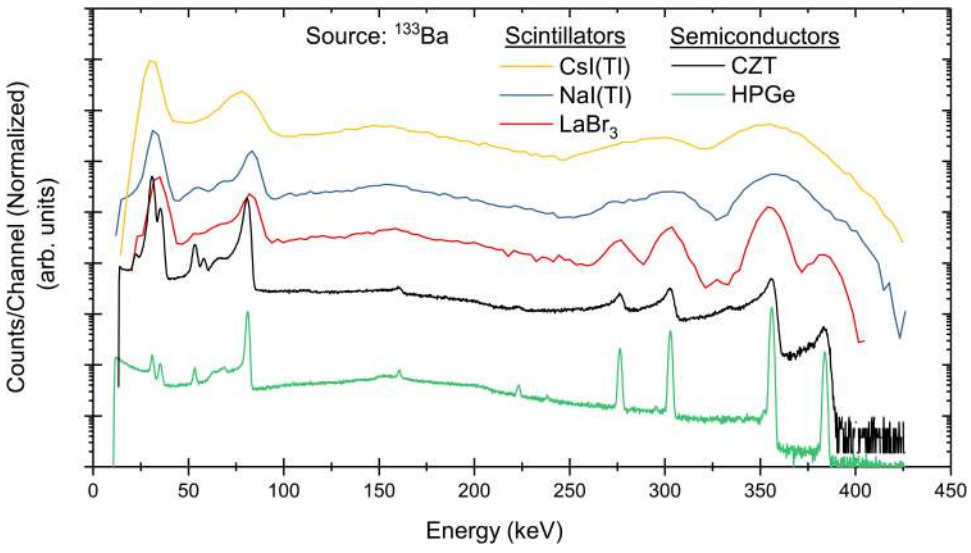

FIG. 1. Comparison of the spectral response from a ^{133}Ba source as produced by a range of commercially available spectrometers. CsI(Tl) (1.27 cm Ø × 3.05 cm), NaI(Tl) (5.08 cm Ø × 5.08 cm), $LaBr_3$ (3.81 cm Ø × 3.81 cm), CZT (0.5 × 0.5 × 0.5 cm^3), and HPGe (6.5 cm Ø × 5 cm) are shown to highlight the differences in resolution between different sensor materials.

Published under license by AIP Publishing.

elements as the basis for such a sensor. Alone, most elements from rows five and six of the periodic table exist as metals, so an additional element(s) is needed to form an ionic-covalent compound with a bandgap wide enough to suppress thermal excitation of electrons, yet still narrow enough to allow for the production of many ionization-induced electron-hole pairs upon a radiation interaction. A bandgap between 1.5 and 2.5 eV is usually suitable for spectrometer applications at room temperature. For this, Se, Br, Te, and I are commonly selected as the appropriate high Z anions that lead to compounds with semiconducting characteristics when bonded with the heavy metals.

In addition to favorable atomic properties, for a semiconducting compound to perform well as a radiation sensor, it must exhibit electronic properties that enable detection limits from ionization-induced charges on the order of fC to pC. As a benchmark posed by Owens, a suitable detector should be able to exhibit a photopeak resolution of 1% or less (at 500 keV) with a volume of 1 cm^3.[7] The key properties for this capability include insulator-level resistivity values (at least $10^8\,\Omega$ cm) that allow for leakage current values lower than several nanoamperes, electron-hole pair creation energies that approach the value of the bandgap, and charge carrier mobilities and lifetimes that enable optimum charge collection efficiency (CCE) (mobility-lifetime product of at least 10^{-5} cm^2/V s). All of these properties are determined by the electronic structure and the bandgap of the compound. Once a gamma ray interacts with the matter composing the semiconductor, the electronic properties dictated by the bandgap determine the magnitude and efficiency by which the signal is generated and collected. To select and develop attractive materials for RTSD applications, it is important to optimize three key electronic properties: resistivity, pair creation energy, and the mobility-lifetime product.

The mobility-lifetime product is particularly important for RTSD materials because it determines the charge collection efficiency (CCE) of a detector. The CCE is expressed in terms of $\mu\tau$ (for parallel-plate geometry[8]) as

$$\mathrm{CCE}(z) = \frac{E(\mu\tau)_e}{d}\left[1 - e^{-(d-z)/(\mu\tau)_e}\right] + \frac{E(\mu\tau)_h}{d}\left[1 - e^{-z/(\mu\tau)_h}\right]. \quad (1)$$

For a given $\mu\tau$ value, charge carriers should be expected to travel an average distance within a certain time before recombination. Because the detection probability of incident gamma rays increases with detector thickness, the ($\mu\tau$) value must be sufficient to allow complete charge transport in thicker detectors.

The output signal from a radiation interaction comes from the movement of electrons and holes inducing charge Q on an electrode. The amplitude of the shaped signal $Q(t)$ produced by a gamma ray is used to determine the timing and energy information from the interaction. Controlling the weighing field and weighing potential experienced by charge carriers is very important to enabling good spectral resolution in RTSD sensors, particularly because the amount of charge induced on an electrode is proportional to weighing potential, $\Delta\Psi$. Samples with parallel-plate electrode geometries are trivial to manufacture and work well when performing simple electrical characterization on crystals. However, the equal weighing potential given to electrons and holes in parallel-plate geometry is detrimental to collecting signals when electrons and holes have differences in mobility.

Consider the following: the total amount of charge induced on an anode in a parallel-plate electrode geometry is expressed as

$$Q_{induced} = \underbrace{q[\psi(x_1) - \psi(x_C)]}_{holes} - \underbrace{\{-q[\psi(x_A) - \psi(x_1)]\}}_{electrons}, \quad (2)$$

where x_1 is the ionization position within the crystal, x_C is the cathode position, and x_A is the anode position. The magnitude of the weighing potential felt by a charge carrier will differ depending on the interaction depth within the crystal. In a perfect crystal, the fact that carriers experience different weighing potential at different interaction positions is irrelevant; all the charge induced at any electrode from any interaction position would be equivalent due to the sum of $\Delta\Psi$ between positive and negative charge carriers. In this idealized case, the charge induced is totally independent of the interaction position within the crystal because both carriers fully induce charge.

However, in a real crystal, this is not the case. Electronic trap states in the bandgap (caused by defects and impurity atoms trap

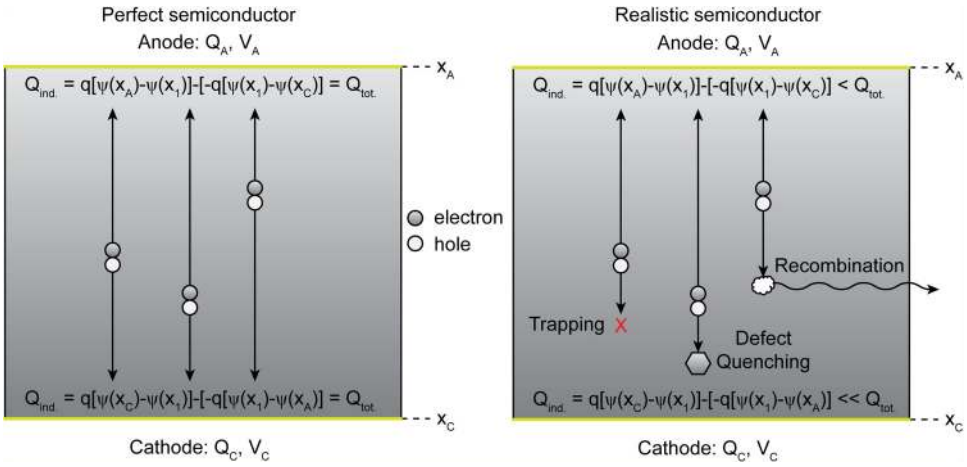

FIG. 2. As electrons and holes transit throughout a semiconductor, they induce charge on the collecting electrode proportional to the difference in weighing potential between the site of their generation and the site of their termination. In a perfect semiconductor (left), the amount of induced charge is equal to the total amount generated in ionization. In a realistic semiconductor (right), effects that quench the charge before it reaches the electrode diminish the total induced charge from the interaction.

Published under license by AIP Publishing.

charges, macroscopic and microstructural defects, quench charge carriers, and stochastic electron-hole recombination) result in the loss of ionization-induced charge. These effects frequently influence one charge carrier more severely than the other, as most RTSD candidates are affected by either the electrons or the holes having significantly better transport properties through the crystal lattice. Because the induced charge on the collecting electrode is determined by the movement of both charged species, signal resolution becomes worse based on the difference in the ability of the two carriers to induce charge at the electrode. An illustration of this phenomenon is shown in Fig. 2. In the case of a perfect semiconductor, the induced charge on the electrode is equal to the total charge generated, while in the realistic case, the induced charge is much less than the total due to an incomplete collection of the minority carrier.

To compensate for these charge collection loss effects, single polarity charge sensing techniques are commonly used to improve resolution in RTSD spectrometers. Variations to the electrode geometry are employed to create a weighing potential distribution that allows the majority charge carrier to undergo a large $\Delta\psi$ as it drifts to the collecting electrode, while the minority carrier undergoes as small a change in $\Delta\psi$ as possible. Because the induced charge is proportional to $\Delta\psi$, it is, therefore, possible to create weighing potential distributions where nearly all of the induced charge is due to the majority carrier, thereby improving the resolution.

The most common electrode geometry design is pixel electrode grids as they enable the lower mobility carrier to have less of a negative influence on the resolution output from a semiconductor detector.[9] If a cathode-electrode geometry is devised where the collecting electrode of the majority charge carrier is made much smaller relative to the size of the minority carrier electrode, the resulting electric field lines will buckle inward. This curvature of the weighting field experienced by charge carriers will create a very high weighing potential change in the vicinity of the pixel used to collect the majority carrier, yet the weighing potential in the remainder of the crystal will remain fairly constant. In this configuration, $\Delta\psi$ for the majority carrier will be very large, whereas $\Delta\psi$ for the minority carrier will be very small. Frisch collars are a similar method of altering the weighing potential throughout the crystal so that the majority carrier undergoes the most potential change. These devices, sometimes referred to as Frisch rings or virtual Frisch grids, were first designed in the early 2000s based on the success of similar designs in gas detectors.[10] Frisch collars are constructed by wrapping a crystal with an insulating dielectric material, which is further wrapped in a conducting metal. The dielectric permittivity and thickness of the insulator separating the metallic collar from the crystal influences the potential profile throughout the semiconductor crystal. The nonlinear weighing potential created by the Frisch collar increases the change in weighing potential experienced by charge carriers generated in the bulk of the detector.

III. OVERVIEW OF RTSD MATERIALS

In addition to featuring exceptional properties in resistivity, pair creation energy, mobility-lifetime product, and physical electron density, an RTSD sensor should feature a defect tolerant crystal structure, a direct bandgap, a thermodynamically stable lattice, chemical and structural stability, and surface properties that allow the formation of Ohmic contacts with electrode metals. To make RTSD sensors economically feasible, they should contain constituent elements that are not scarce and feature precursor compounds that are easily synthesized. Additionally, it is desirable for RTSD materials to melt congruently at low temperatures for ease of large volume crystal growth. These diverse and stringent requirements needed for a material to operate as an RTSD limit the number of candidates of interest that receive attention and undergo focused research and development efforts. Despite this, semiconductor gamma-ray sensor development is a thriving research field. Notably, the past five years have seen a surge in activity within the RTSD development community. A number of review articles have been prepared on RTSD applied materials, including, over the last decade, the review papers by McGregor and Hermon,[11] Owens and Peacock,[12] Luke and Amman,[13] Sellin and Vaitkus,[14] Zaletin and Varvaritsa,[15] and Milbrath *et al.*,[4] as well as the books by Owens,[7] Awadalla,[16] and Iniewski.[17] However, in the last few years, a number of new compounds with stunning potential as RTSD materials have emerged.

Table I summarizes a list of the relevant properties that are reported for the top materials considered for RTSD applications. A thorough literature review was performed to summarize the best-reported properties for each of the 51 compounds listed; however, it cannot be discounted that there exists better performance for any of the compounds in the table. Pair creation energies given in parentheses were calculated from the empirical formula given by Alig and Bloom[35] as

$$\varepsilon = 2.73E_g + 0.55. \tag{3}$$

In Table I, values with n.r. are not reported in the literature, and compounds in bold have seen focused research and development within the last ten years. In Secs. III A and III B, each group or family of compounds is discussed in detail.

A. CdTe compounds, TlBr, and HgI_2

Among all semiconducting compounds with attractive physical and electronic properties, CdTe and CdZnTe (CZT) are the forefront of RTSD sensor materials. In fact, it is very rare to find a paper on an emerging detector candidate material that does not compare itself to CZT. When it was discovered in the 1950s that CdTe platelets were sensitive to excitation from charged particles, it became one of the first semiconducting compounds investigated for particle detection. It is now common to alloy Zn into the crystal to increase the bandgap and prevent polarization effects from occurring after long periods under bias.[90] Today, the premier semiconductor material for ambient temperature radiation sensing applications is <15% Zn-doped CdTe, which features a bandgap around 1.57 eV (for 10% Zn-doped) at 300 K and resistivity improved 1–2 orders of magnitude over pure CdTe.[91] With modern charge sensing and depth of interaction correction techniques, it is possible for CZT to exhibit photopeak resolution well below 1% at 662 keV.[92–94] The intensive development of CZT has enabled it to feature some of the best-combined properties of all compounds listed

Published under license by AIP Publishing.

TABLE I. Electronic properties of candidate RTSD materials as reported in the literature. Value references taken from Owens and Peacock[12] along with sources are given in column 2. Compounds in bold have seen focused research and development within the last ten years.

Material	References	Bandgap (eV)	Resistivity (Ω cm)	$(\mu\tau)_e$ (cm^2/V)	Spectroscopic response?	Pair creation energy
CdTe	18 and 19	1.44	1×10^{9}	$1–2 \times 10^{-2}$	Yes	4.43
CdZnTe	20 and 21	1.57	$10^{9}–10^{10}$	7.5×10^{-3}	Yes	4.64
HgI_2	7	2.15	1×10^{13}	3×10^{-4}	Yes	4.20
TlBr	22 and 23	2.68	1×10^{10}	3×10^{-3}	Yes	6.50
CdMnTe	24–27	1.61	3×10^{10}	7×10^{-3}	Yes	2.12
CdSe	28 and 29	1.73	1×10^{12}	6.3×10^{-5}	Yes	5.50
CdZnSe	30	2.00	2×10^{10}	1×10^{-4}	No	6.00
CdTeSe	31 and 32	1.47	5×10^{9}	4×10^{-3}	Yes	(4.56)
GaAs	33	1.42	1×10^{8}	8×10^{-5}	Yes	4.20
GaSb	34	0.72	n.r.	3×10^{-5}	Yes	(2.51)
GaSe	35–37	2.03	$10^{8}–10^{10}$	3.7×10^{-5}	Yes	4.49
GaTe	37	1.66	1×10^{9}	n.r.	No	(5.08)
GaN	15	3.40	1×10^{11}	1×10^{-4}	No	10.2
GaP	15	2.26	1×10^{9}	1×10^{-5}	No	7.00
InP	38	1.34	1×10^{9}	5×10^{-6}	Yes	4.20
AlSb	39	1.65	1×10^{8}	1.2×10^{-4}	No	4.71
$TlHgInS_3$	40	1.74	4×10^{9}	3.6×10^{-4}	No	(5.30)
$Cs_2Hg_6S_7$	41 and 42	1.63	6×10^{7}	1.7×10^{-3}	Yes	(4.99)
$CsHgInS_3$	43	2.30	9×10^{10}	3.6×10^{-5}	No	(6.83)
$TlGaSe_2$	44	1.93	1×10^{9}	6×10^{-5}	No	(5.82)
$AgGaSe_2$	45	1.70	1×10^{11}	6.0×10^{-6}	No	(5.19)
$TlInSe_2$	46–48	1.10	$10^{6}–10^{7}$	1×10^{-2}	No	3.60
$LiInSe_2$	49 and 50	2.85	1×10^{11}	3.0×10^{-6}	No	(8.33)
$LiGaSe_2$	51	2.80	1×10^{8}	n.r.	No	(8.19)
$CsCdInSe_3$	52	2.40	4×10^{9}	1.2×10^{-5}	No	(7.10)
Tl_3AsSe_3	53	n.r.	$10^{6}–10^{7}$	n.r.	No	n.r.
$Cs_2Hg_3Se_4$	54	2.1	1.1×10^{9}	8.0×10^{-4}	No	(6.28)
$Pb_2P_2Se_6$	55 and 56	1.88	5×10^{11}	3.1×10^{-4}	Yes	(5.68)
$Cu_2I_2Se_6$	57	1.95	10^{12}	n.r.	No	(5.87)
$CsCdInTe_3$	52	1.78	2×10^{8}	1.1×10^{-4}	No	(5.06)
$Cs_2Cd_3Te_4$	54	2.5	1×10^{6}	1.1×10^{-4}	No	(7.38)
PbI_2	7	2.32	1×10^{13}	1×10^{-5}	Yes	4.90
InI	58 and 59	2.00	1×10^{11}	7×10^{-5}	Yes	(6.01)
SbI_3	60	2.20	1×10^{10}	n.r.	No	(6.56)
BiI_3	61 and 62	1.67	$10^{8}–10^{11}$	1×10^{-4}	Yes	5.80
β-$Hg_3S_2Cl_2$	63	2.56	1×10^{10}	1.4×10^{-4}	No	(7.54)
$CsPbBr_3$	64	2.25	$10^{9}–10^{11}$	1.7×10^{-3}	Yes	(6.69)
$Hg_3Se_2Br_2$	65	2.22	1×10^{11}	1.4×10^{-4}	Yes	(6.56)
SbSeI	66	1.70	1×10^{8}	4.4×10^{-4}	No	(5.19)
Tl_4CdI_6	67	2.80	2×10^{10}	6.1×10^{-4}	Yes	(8.19)
Tl_6SI_4	68	2.04	1×10^{10}	2.1×10^{-3}	Yes	(6.12)
Tl_6SeI_4	69	1.86	4×10^{12}	7.0×10^{-3}	Yes	(5.63)
Tl_4HgI_6	53	n.r.	$10^{11}–10^{12}$	8.0×10^{-4}	Yes	n.r.
$TlSn_2I_5$	70	2.14	4×10^{10}	1.1×10^{-3}	No	(6.39)
$Hg_3S_2I_2$	71	2.25	2×10^{11}	1.6×10^{-6}	No	(6.69)
$Hg_3Se_2I_2$	71	2.12	1.2×10^{12}	1.0×10^{-5}	Yes	(6.34)
$Hg_3Te_2I_2$	71	1.93	3.5×10^{12}	3.3×10^{-6}	No	(5.82)
$Rb_3Bi_2I_9$	72	1.93	3.2×10^{11}	1.7×10^{-6}	No	(5.82)
$Rb_3Sb_2I_9$	72	2.03	8.5×10^{10}	4.5×10^{-6}	No	(6.09)
$Cs_3Bi_2I_9$	72	2.06	9.4×10^{12}	5.4×10^{-5}	No	(6.17)
$Cs_3Sb_2I_9$	72	1.89	5.2×10^{11}	1.1×10^{-5}	No	(5.71)
$CdGeAs_2$	73	0.9–1.0	$10^{7}–10^{9}$	n.r.	No	(3.30)

Published under license by AIP Publishing.

TABLE I. (*Continued.*)

Material	References	Bandgap (eV)	Resistivity (Ω cm)	$(\mu\tau)_e$ (cm^2/V)	Spectroscopic response?	Pair creation energy
LiZnAs	74 and 75	1.51	10^6–10^{11}	n.r.	No	(4.67)
LiZnP	74 and 76	2.04	10^6–10^{11}	n.r.	Yes	(6.12)
4H-SiC	15 and 77	3.27	2×10^{12}	4×10^{-4}	Yes	7.78
Diamond	78 and 79	5.47	5×10^{14}	2.7×10^{-7}	No	13.0
PbO	80	2.80	1×10^{13}	1×10^{-8}	No	(8.19)
ZnO	81	3.30	3×10^{13}	10^{-6}–10^{-4}	No	(8.37)
$MAPbI_3$	82–84	1.54	10^8–10^9	1.0×10^{-2}	Yes	(4.75)
$FAPbI_3$	82, 85, and 86	1.43	10^6–10^9	1.8×10^{-2}	Yes	(4.40)
$FACsPb(BrI)_3$	86	1.52	10^8–10^9	1.2×10^{-1}	Yes	(4.69)
$MAPb(BrI)_3$	82	n.r.	n.r.	1.0×10^{-5}	Yes	n.r.
$MAPbBr_3$	87 and 88	2.3	1.7×10^7	1.2×10^{-2}	No	(6.83)
$MAPbBr_3$:Cl	89	2.3	3.6×10^9	1.2×10^{-2}	Yes	(6.83)

in Table 1. Additionally, there are many commercially available gamma-ray detection systems based on the material for applications in nuclear security, medical imaging, and astrophysics.[95] Review papers on CdTe and CZT from Scheiber and Chambron,[96] Eisen and Shor,[97] and Del Sordo *et al.*,[91] among others, can be read for details on the development of the materials.

Despite the development and success of CZT as an RTSD sensor, several intrinsic material issues limit its performance at detecting gamma rays. The first category of complications in CZT comes from structural defects that are seen in the form of twinning, stacking faults, and grain boundaries. As highlighted by Triboulet and Siffert in their book on the subject,[98] CdTe is vulnerable to defect formation in several ways. Low thermal conductivity, low critical-resolved shear stress, differences in stability between the sphalerite and wurtzite structures, retrograde solubility, and the high symmetry of the sphalerite phase give CZT a predisposition to feature a high density of dislocations, twins, grain boundaries, and secondary phase precipitation. The second category of CZT issues, and perhaps the more difficult to solve, is the presence of the secondary phases that arise during growth. During the growth process, Te inclusion particles and Te precipitates segregate within the crystal as a separate phase. Particles are believed to form via the melt-droplet capture method at grain boundaries or defect sites on the solid-liquid interface,[99] while precipitates form due to a retrograde solubility phenomenon that causes noncongruent melting of the CdTe liquid phase.[100] Transmission infrared micrographs from a CZT sample are presented in Fig. 3 to show examples of the structural defects and Te precipitates that are found throughout bulk crystals. Because the Te defect phases can quench the charge generated in ionization from gamma rays, detector crystals must be meticulously harvested from pristine sections of the boule.[101] In addition to the struggles this material faces from its structure, the cost of CdTe and CZT is also a point of concern for large-scale production. Due largely to the scarcity of Te, the production costs of RTSD detectors composed of the element can be high.[102]

Despite the challenges posed by the defect and inclusion issues in CZT, a large amount of research have been undergone to

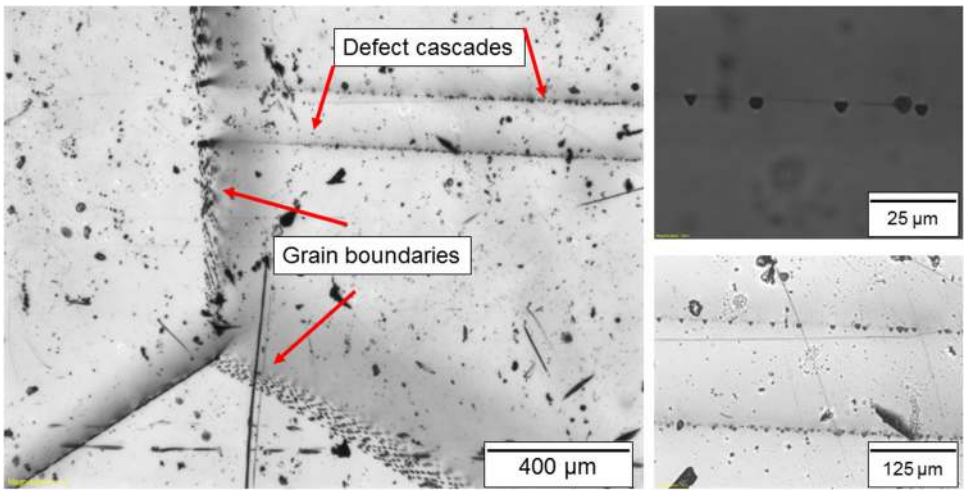

FIG. 3. IR micrographs showing the Te inclusions that populate the bulk of CZT crystals due to retrograde solubility during crystal growth (sample courtesy of Dr. Mary Bliss, PNNL).

Published under license by AIP Publishing.

mitigate such problems and make CZT the success it is today. Furthermore, the utilization of 2D and 3D depth correction techniques can compensate for many of the material limitations and in the best cases enable spectral resolution in crystals with Te inclusions to approach that of a defect-free environment. Advanced and tailored crystal growth techniques, such as the boron oxide encapsulated vertical Bridgman method,[103] have been developed to enable the growth of large single crystal grains with etch pit densities on the order of 10^{-3}/cm^2. Thermal annealing under excess Cd vapor pressure has been found to reduce the size and density of Te inclusions by over an order of magnitude.[104,105] Additionally, bandgap trap states caused by various defects are very well understood in CZT. To electrically compensate for charged trap states caused by native defects, CdTe is often grown with engineered dopants such as Cl, Al, or In to incorporate on vacancies on the Cd or Te sites.[18,106] In materials such as CdTe:Cl and CdTe:In, compensation dopants on the order of 1–2 ppm are added to increase the resistivity of the crystal.[107] Through growth, processing, and treatment techniques such as these, commercially available CZT instruments are produced and are able to acquire room temperature gamma-ray spectra with good performance.

Due to the success of Zn-doped CdTe, a number of other CdTe alloys have been investigated for their performance as RTSDs. CdMnTe (CMT) has been one of the most successfully developed of these alloyed compounds. As Mn is introduced into the CdTe crystal lattice, it increases the bandgap by about twice the amount that Zn does, which (when the crystal is compensated with dopants such as V or In) enables resistivity values greater than that of CZT.[25] In addition to the wider bandgap, the segregation coefficient of CMT is much closer to unity than CZT and allows for a more homogenous elemental distribution in Bridgman-grown crystals. Due to these qualities, CMT has been demonstrated to exhibit exceptional detector performance. Recently, Kim *et al.* showed a resolution of 2.1% at 662 keV and 1.5% at 1.27 MeV from >1 cm thick CMT detectors equipped with Frisch grid electrode patterning.[27] However, like CdTe and CZT, CMT performance is also held back by the presence of Te inclusions and precipitates.[108] Despite the inherent crystal problems, CMT is an exciting material to follow as its development for RTSD applications continues.

Efforts to develop similar compounds to CdTe with improved performance have also been explored by changing the Te anion to Se. CdSe features a naturally wider bandgap due to the smaller atomic radius of Se relative to Te, which enables CdSe crystals to exhibit a much higher resistivity. One of the most attractive features of CdTe is the total lack of polarization phenomena exhibited by the compound, which allows for stable count rates after extended periods under bias without the need for a polarization-compensating dopant.[29] Similarly, alloying together both CdTe and CdSe yields a compound that performs expectedly well as a radiation sensor. CdTeSe (10% Se-alloyed) has shown remarkable $(\mu\tau)_e$ values, up to the order of 10^{-3} cm^2/V, as well as demonstrated gamma-ray spectra from the 59 keV emission of ^{241}Am.[109]

TlBr is another pervasive material that has shown tremendous promise for RTSD applications. The physical and atomic properties of TlBr are exceptional for radiation detection, as its density is among the highest of RTSD candidates at 7.56 g/cm^3, and its bandgap of 2.56 eV maximizes resistivity at the cost of slightly higher pair creation energy. TlBr was among the first semiconducting materials demonstrated for radiation counting in 1947;[110] however, modern development of the material for gamma-ray spectroscopy began in the late 1980s.[111] Because it is a congruently melting compound with a relatively low melting temperature of 460 °C, TlBr can be grown with relative ease in large volumes. Additionally, while it has a softer lattice due to its ionic nature, TlBr does not feature intrinsic structural defects like crystals in the CdTe family. While the mobility-lifetime product of the material surpasses 10^{-3} cm^2/Vs, the mobility of electrons in TlBr is lower than most candidate RTSD materials. The remarkable lifetime of both electrons and holes (between 1 and 10 μs[112] allows them to perform with similar mobility-lifetime values to that of CZT.

Like most semiconductors, TlBr features some degree of bandgap trap states from point defects. Fortunately, the dominant defects are electrically neutral and pin the Fermi level near the middle of the bandgap that helps maintain high resistivity in the crystal.[113] One of the other main drawbacks in TlBr historically has been polarization that leads to the degeneration of electronic performance after extended periods under bias.[114] However, by engineering the crystals with Tl contacts, this issue has been solved.[115] Today, both pixelated[116] and capacitive Frisch grid detectors[117] have demonstrated a resolution of <1% at 662 keV. Examples of single pixel prototype TlBr detectors are presented in Fig. 4.

The final product of the highly developed RTSD materials is HgI_2, shown in Fig. 5. The first application of HgI_2 as a gamma-ray spectrometer came in 1971,[118] and through the following 45 years, it has been developed into a quality gamma-ray sensor. Early attempts to produce gamma-ray spectra with HgI_2 proved challenging due to the hole $(\mu\tau)$ product lagging orders of magnitude behind that of electrons. Due to this, the charge induced on an electrode from a gamma-ray interaction has a strong dependence on the location within the crystal where the interaction takes place. Photopeak resolution suffers when equal importance is given to electrons and holes for forming the signal from radiation interactions. A remedy for this problem is found by engineering electrode geometries that allow electrons to induce the majority of charge from a radiation interaction. Baciak and He were able to demonstrate 1.55% resolution for the 662 keV gamma ray of ^{137}Cs by collecting charge from pixelated anode electrodes and performing depth correction on interaction signals.[119] Spectra reconstructed from single depths of interaction were demonstrated to exhibit remarkable 662 keV resolution of 1.06%. Likewise, Ariesanti *et al.* were able to demonstrate 1.8% energy resolution by utilizing Frisch collars to control the weighing potential of electrons and holes.[120]

B. Recent promising RTSD materials

As discussed above, the highest tier of developed RTSD materials consists of CdTe, CZT, TlBr, and HgI_2. However, in addition to those compounds, dozens of materials with promising atomic and electronic properties exist, which could, given enough development, emerge as state of the art.

1. Chalcogenides

Many of the emerging RTSD compounds have been identified by the dimensional reduction concept posed in the work by

Published under license by AIP Publishing.

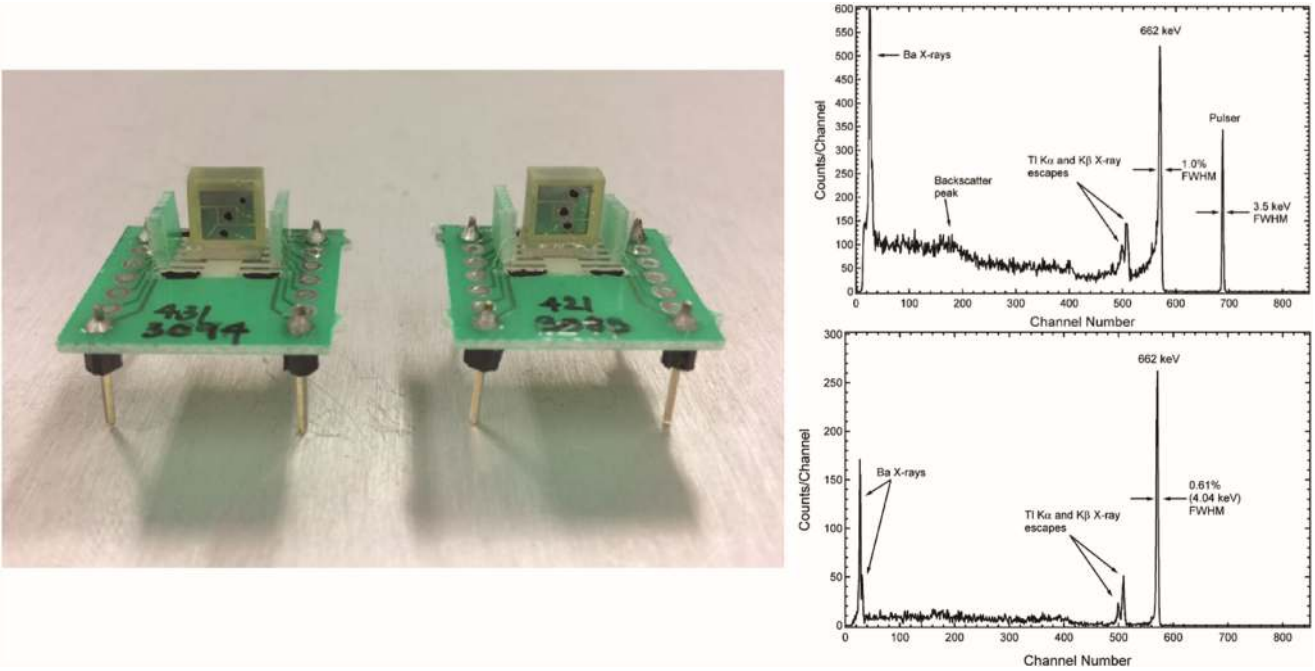

FIG. 4. Prototype TlBr single pixel detectors with Tl electrodes mounted to an IC substrate (sample courtesy of Dr. Keitaro Hitomi, Tohoku University). Spectra shown depict ^{137}Cs signals obtained from capacitive Frisch grid TlBr detectors without (top) and with (bottom) depth correction applied. Reprinted with permission from Hitomi *et al.*, IEEE Trans. Nucl. Sci. **60**(2), 1156–1161 (2013). Copyright 2013 IEEE.

Androulakis *et al.*[54] These materials are mainly ionic and can be classified as either chalcogenides that are based on the anions S (Z = 16), Se (Z = 34), and Te (Z = 51) or chalcohalides that are based on the anions Cl (Z = 17), Br (Z = 35), and I (Z = 53). With the selection of heavy-Z cations, even compounds based on the lighter cations S and Cl can achieve high electron densities and become extremely efficient radiation detectors. Recently, a number of ternary chalcogenide materials have emerged as exceptionally

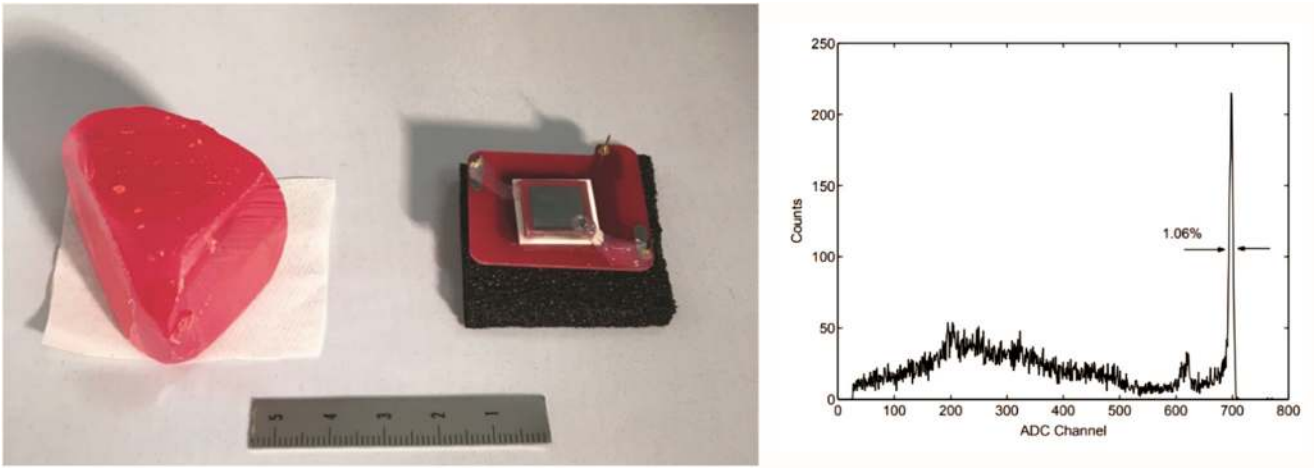

FIG. 5. A 1.2 kg ingot of HgI_2 (left) along with a single crystal section of the material fashioned into a prototype detector (right) (sample provided by Constellation Technology Corporation). The spectrum shown presents a ^{137}Cs signal obtained from a HgI_2 detector with depth correction applied. Reprinted with permission from Baciak and He, Nucl. Instrum. Methods Phys. Res. A **505**(1–2), 191–194 (2003). Copyright 2003 Elsevier.

Published under license by AIP Publishing.

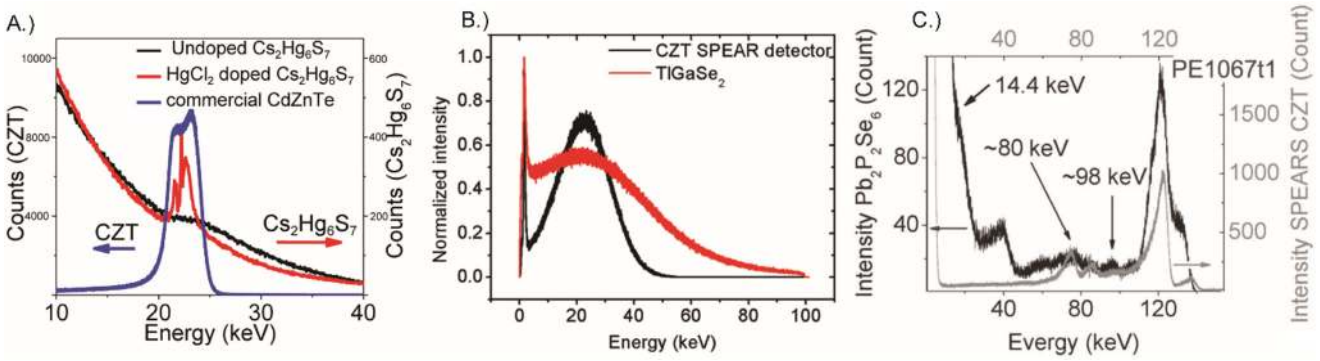

FIG. 6. Spectra from chalcogenide compounds. (a) shows the response of $Cs_2Hg_6S_7$ to unfiltered Ag x-ray radiation. Reprinted with permission from Li *et al.*, Cryst. Growth Des. **12**(6), 3250–3256 (2012). Copyright 2012 American Chemical Society. (b) shows the response of $TlGaSe_2$ to the same. Reprinted with permission from Johnsen *et al.*, Chem. Mater. **23**(12), 3120–3128 (2011). Copyright 2011 American Chemical Society. (c) compares the ^{57}Co spectra of $Pb_2P_2Se_6$ to a commercial CZT SPEAR detector. Reprinted with permission from Wang *et al.*, Adv. Funct. Mater. **25**(30), 4874–4881 (2015). Copyright 2015 John Wiley and Sons.

attractive materials for applicability in RTSD devices. Figure 6 provides spectra collected from some of the emerging chalcogenide RTSD materials.

Chalcogenides based on sulfur have received attention for RTSD applications and are in some cases very promising detector materials. The first of these compounds is $TlHgInS_3$. Because it is an incongruent melting compound, $TlHgInS_3$ is best synthesized through a direct combination reaction followed by controlled freezing to yield a single-phase material. Despite the difficulty level of its synthesis, the compound yields good $(\mu\tau)$ and a resistivity of $\sim 10^{-4}$ cm^2/V and $\sim 10^9\ \Omega$ cm, respectively. Thus far, $TlHgInS_3$ has shown only current mode responses to pulsed x-rays.[40] $Cs_2Hg_6S_7$ likewise has very high $(\mu\tau)_e$ values, on the order of 10^{-3} cm^2/V, despite low resistivity on the order of 10^6–$10^7\ \Omega$ cm.[41,42] Peters *et al.*[121] have reported weakly resolved ^{57}Co spectra measured with $Cs_2Hg_6S_7$, with the poor resolution attributable to the low resistivity caused by native defects within the samples.[122] Toward improving RTSD performance, it has been shown that Cd, Cl, and In dopants can be incorporated into the $Cs_2Hg_6S_7$ synthesis to reduce defect centers and increase the crystal's resistivity and $(\mu\tau)_e$.[41,42] The final sulfur based chalcogenide that has been investigated for RTSDs is $CsHgInS_3$. Due to its complicated layered structure, $CsHgInS_3$ exhibits anisotropy in the electrical properties measured in the (001) orientation to that of the transverse orientations. $CsHgInS_3$ does not melt congruently; however, it has been grown into sufficiently sized single crystals through the travelling heat method growth.[43] It exhibits the best resistivity of the S-based chalcogenides, on the order of nearly $10^{11}\ \Omega$ cm, but one of the worst $(\mu\tau)_e$ values, on the order of 10^{-5} cm^2/V.[43]

Se-based chalcogenide materials are one of the largest RTSD material groups being investigated and include the compounds $AgGaSe_2$, $TlGaSe_2$, $TlInSe_2$, $LiInSe_2$, $LiGaSe_2$, Tl_3AsSe_3, $CsCdInSe_3$, $Cs_2Hg_3Se_4$, and $Pb_2P_2Se_6$. A few of these compounds can be subcategorized as members of a group with the $ABSe_2$ structure, some of which are classified as chalcopyrites. The chalcopyrite compound $AgGaSe_2$ has shown response to alpha particles and (nonspectroscopic) response to gamma rays due to the low, but equal magnitude, values of $(\mu\tau)_e$ and $(\mu\tau)_h$ it exhibit.[45] Roy *et al.* have posed to use the compound as a solid-state thermal neutron detector due to the 68 b thermal cross section of natural Ag.[45] Recent improvements to large volume crystal growth make $AgGaSe_2$ an interesting compound to revisit for detector development.[123] $TlGaSe_2$ is a layered and highly anisotropic compound that features a difference in the resistivity of $10^5\ \Omega$ cm when measured between the in-plane and transverse orientations. Despite this large anisotropy, resistivity on the order of $10^9\ \Omega$ cm and $(\mu\tau)$ products in the 10^{-5} cm^2/V range have been achieved in Bridgman-grown samples.[44] At this point, $TlGaSe_2$ has reported only nonspectroscopic results from high intensity x-ray sources, but the unusually low resistivity for its ~2 eV bandgap indicates that further improvement in the material is possible.

Three of the Se-based chalcogenide compounds have received a particular emphasis on RTSD development, due largely to their potential as alternative neutron sensors to ^3He. The highly anisotropic and chainlike structured $TlInSe_2$ is an interesting candidate for solid-state neutron detectors because it contains the isotope ^{115}In, which constitutes 95.7% of natural In. The indium present in these detectors undergoes $^{115}In(n,\beta)^{116}Sn$ reactions that have high thermal neutron cross sections of 200 b. Alekseev investigated $TlInSe_2$ for such applications and found that $10^6\ \Omega$ cm resistive crystals exhibited a sensitivity of 10^{-13} A/n cm^2 s when operating the detector in current mode and also found that a ^6Li filter could successfully shield neutrons from the signal for pulse shaping purposes.[46] Pulse mode operation of a $TlInSe_2$ detector has demonstrated promising, but nonspectroscopic, response to a number of neutron and gamma sources, with present limitations possibly due to the material's low $(\mu\tau)$ products (in the 10^{-6}–10^{-5} cm^2/V range).[50] Even more sensitive to neutrons is the compound $LiInSe_2$, which contains ^{115}In as well as ^6Li, which has a 940 b $^6Li(n,\alpha)^3H$ thermal neutron cross section. $LiInSe_2$ is also a much more electronically promising compound. It has exhibited a resistivity of $10^{11}\ \Omega$ cm, good carrier mobility, and responsivity to alpha particles, gamma rays, and neutrons.[49,124] The compound does suffer from a number of deep level trap states that promote carrier recombination,[125] and precipitation of defects

Published under license by AIP Publishing.

within the bulk matrix limits charge collection efficiency.[126] Interestingly, these recombination centers make $LiInSe_2$ one of the few compounds that can detect radiation through both solid-state charge generation as a semiconductor, as well as by producing scintillation light that can be read out by a photodiode.[127] The last of the Se-based neutron detecting chalcogenides, $LiGaSe_2$, has shown resistivity on the order of $10^8\,\Omega\,cm$ but also exhibits very poor charge mobility properties that leave it unresponsive to photoconduction.[124] Potentially contributing to this are the number of oxide and carbide defects identified in the compound.[51] Stowe *et al.* demonstrated that resistivity could be increased to $10^{10}\,\Omega\,cm$ by annealing $LiGaSe_2$ in the presence of Li;[51] however, pulse mode operation has yet to be demonstrated by the material. Finally, Wiggins *et al.* investigated alloys of $LiGaSe_2$ and $LiInSe_2$ of the form $LiIn_xGa_{1-x}Se_2$. The alloyed material was designed as a scintillation neutron detector and was able to resolve spectra from alpha particles.[128]

Nonchalcopyrite chalcogenides based on Se anions are often more complex than their counterparts. The compound Tl_3AsSe_3 has demonstrated nonspectroscopic radiation response after long counting times but is still limited in its development due to a low resistivity of $10^6\,\Omega\,cm$.[53] Growth using a high purity starting material has yielded resistivity up to $\sim 10^8\,\Omega\,cm$ (reported as MΩ/m AC), but the compound has yet to demonstrate spectral response.[129] The layered compound $CsCdInSe_3$ is another promising chalcogenide material that can be grown via the Bridgman method. Despite its large bandgap of 2.8 eV, the resistivity of this compound is only in the $10^9\,\Omega\,cm$ range, indicating the presence of some phenomena increasing dark current. The measured $(\mu\tau)_e$ values are on the low-$10^{-5}\,cm^2/V$ order, which has prevented the material from exhibiting a response to gamma rays.[52] Care needs to be taken to store $CsCdInSe_3$, as oxidation onsets in the presence of air. The compound $Cs_2Hg_3Se_4$ was investigated by Androulakis *et al.* as an example of the dimensional reduction process for identifying candidate detector materials.[54] $Cs_2Hg_3Se_4$ exhibited an impressive resistivity of $10^9\,\Omega\,cm$ as well as competitive $(\mu\tau)_e$ at the high end of the $10^{-4}\,cm^2/V$ range.

Single crystals of $Pb_2P_2Se_6$ grown by the Bridgman method have been shown to exhibit resistivity on the order of $10^{10}\,\Omega\,cm$, $(\mu\tau)_e$ values in the $10^{-5}\,cm^2/V$ range, and an 8.2% resolution from the 122 keV gamma-ray emission of ^{57}Co in the first reported investigation of the compound.[55] Subsequent development of the material reported an order of magnitude increase to resistivity and $(\mu\tau)_e$ values to $10^{11}\,\Omega\,cm$ and $10^{-4}\,cm^2/V$, respectively.[56] The reported drawback to the performance of $Pb_2P_2Se_6$ has been the reproducibility in the performance of the material due to its sensitivity to oxygen defects. Kostina *et al.* reported low electron mobility of $10\,cm^2/V\,s$ due to deep level traps that were ascribed to oxygen incorporation into the crystal.[130] Despite this, $Pb_2P_2Se_6$ is one of the more promising emerging RTSD candidate materials to date.

Chalcogenide compounds of RTSD interest based on the Te anion include $CsCdInTe_3$, $LiGaTe_2$, and $Cs_2Cd_3Te_4$. Despite their heavier atomic components, which is a benefit for photon detection efficiency, the Te-based compounds are generally at a lower development level than the lighter Se-based chalcogenides. Tupitsyn *et al.* reported that $LiGaTe_2$ was troublesome to synthesize and was not able to electronically characterize the material.[124] Better behavior was found for $CsCdInTe_3$, which is an isomorph with the layer-structured $CsCdInSe_3$. However, while $CsCdInTe_3$ features a lower resistivity and smaller bandgap that enables better $(\mu\tau)_e$ behavior,[52] it has yet to show any response to radiation. Finally, the compound $Cs_2Cd_3Te_4$ was, like $Cs_2Hg_3Se_4$, investigated by Androulakis as a demonstration of the dimensional reduction technique to identify attractive RTSD candidates.[54] Despite its sufficiently large 2.1 eV bandgap, $Cs_2Cd_3Te_4$ exhibited resistivity on the low end at $10^6\,\Omega\,cm$ but did possess attractive $(\mu\tau)_e$ values on the order of high-$10^{-4}\,cm^2/V$.

2. Iodides and chalcohalides

Because of the high Z_{eff} criteria needed for good detection efficiency, the heaviest of the ionic compounds designed for radiation sensor applications are built around iodine as the anion. Many iodide compounds have bandgaps that are greater than the threshold needed to make compounds semiconducting in nature; however, several of these compounds are still quite important for radiation detection and include famous scintillating compounds such as NaI and CsI. Examples of spectra from iodide RTSD compounds, excluding HgI_2 which was discussed prior, are included in Fig. 7.

Apart from HgI_2, the most prevalent iodide compound investigated as an RTSD candidate is PbI_2. Backed by its wide bandgap of 2.32 eV, PbI_2 routinely exhibits a resistivity of about $10^{12}\,\Omega\,cm$ or more. Its initial demonstration as a particle detector was by Roth and Willig in 1970,[133] who noted that despite its unmeasurably high resistivity (due to instrument precision at the time) and low $(\mu\tau)_e$ value of $10^{-8}\,cm^2/V$, platelets of the crystal responded well to the x-rays of ^{55}Fe. Since then, gamma-ray spectra from sub-100 keV sources have been obtained from PbI_2 sensors by Shah *et al.*,[131] Shoji *et al.*,[134] Zhu *et al.*,[135] and Deich and Roth.[136] Sheets of PbI_2 have been proven exceptional for use as x-ray detectors, where detection of the lower energy x-ray radiation is not jeopardized by the thickness-related challenges of the detector.[131,137–139] PbI_2 has also been demonstrated as a potential photodetector material and has been able to convert scintillation from $Lu_4O_{12}Si_3$ and CsI(Na) scintillators into gamma-ray spectra.[140]

Due to its attractive bandgap of 2.0 eV, InI has also received some interest as an RTSD over the past 20 years. Both Shah *et al.*[141] and Onodera *et al.*[59] reported gamma-ray spectra from crystals of this material. Riabov reported an exceptional resistivity of up to $10^{12}\,\Omega\,cm$ by using Ti electrodes; however, it was also posed that the high resistivity readings could have arisen from contact resistance created by an oxide layer.[142] InI also features inclusion-type defects that draw similarities to the Te inclusions in CdTe. Despite its demonstrated potential, good resolution gamma-ray spectra have yet to be achieved for the material; however, growth and processing improvements could likely unlock better spectral performance.

Apart from HgI_2, PbI_2, and InI, the compound BiI_3 has received significant development for RTSD use. Its potential application as a detector began to be realized in 1995, when Nason and Keller investigated a detector crystal grown by physical vapor transport assisted by a BiI_3 seed.[143] In 1999, Dmitriyev *et al.*[144] released a study on the optical and electronic properties of BiI_3 relevant to utilizing it as a radiation sensor, and finally, in 2001, Matsumoto *et al.*[145] released the first paper presenting BiI_3 as a

Published under license by AIP Publishing.

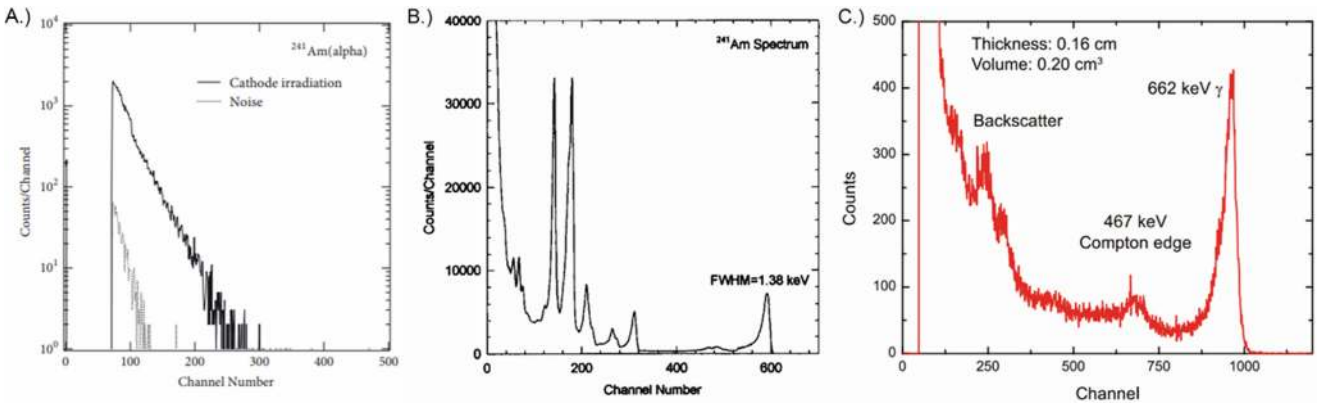

FIG. 7. Spectra from iodide compounds intended for RTSD application. Spectrum (a) shows a signature of ^{241}Am obtained from a SbI_3 detector [From Onodera *et al.*, *Evaluation of Antimony Tri-Iodide Crystals for Radiation Detectors*. Copyright 2018 Onodera *et al.*, licensed under a Creative Commons Attribution License. Reprinted with permission from Science and Technology of Nuclear Installations], (b) shows a ^{241}Am spectrum obtained from PbI_2 [Reprinted with permission from Shah *et al.*, Nucl. Instrum. Methods Phys. Res. A **380**(1), 266–270 (1996). Copyright 1996 Elsevier], and spectrum (c) shows a ^{137}Cs signal obtained from BiI_3 [Reprinted with permission from Johns *et al.*, Appl. Phys. Lett. **109**(9), 092105 (2016). Copyright 2016 AIP Publishing].

material capable of response to radiation. BiI_3, a layered structure like many other binary iodide crystals, exhibits best-reported resistivity and $(\mu\tau)$ values of $10^{10}\,\Omega\,cm$ and $10^{-4}\,cm^2/V$, respectively. Han *et al.*[146] and Gokhale *et al.*[147] investigated the effects of alloying SbI_3 into BiI_3 crystals, which they found to enhance electronic properties and the resistance of the compound to polarization after extended periods of bias. The Sb:BiI_3 crystals were the first reported to respond to gamma rays and produced a resolution of 7.5% from the 59.5 keV emission of ^{241}Am.[147]

BiI_3, and Sb:BiI_3, exhibited poor response to gamma rays until the discovery of void inclusions within melt-grown samples was linked to the deterioration of charge transport capabilities.[132,148,149] Crystals wherein void inclusions were suppressed have shown the ability to resolve gamma-ray spectra from a number of sources, with a best-reported resolution of 2.2% for the 662 keV emission of ^{137}Cs.[132] The soft, layered lattice of BiI_3 makes it particularly susceptible to deformation, which negatively impacts resistivity and enhances the sample-to-sample variations in electronic properties.[149] Recently, Saito *et al.* explored iodine annealing as a post-processing step to compensate iodine vacancies in the lattice and showed an improvement in resistivity to $10^{11}\,\Omega\,cm$ following the I_2 anneal.[62] With its low toxicity, ease of growth, favorable properties, and good resolution demonstrated toward high-energy gamma rays, BiI_3 is an attractive compound for future RTSD development. SbI_3 single crystals have also recently been investigated by Onodera *et al.* as an RTSD candidate.[60] SbI_3 is an attractive compound due to its low melting point at 171 °C and high resistivity on the order of $10^{10}\,\Omega\,cm$. The promising first studies on this material as a radiation sensor have shown response to alpha particles and some non-spectroscopic response to ^{137}Cs gamma rays.[60]

Chalcohalides are ternary compounds based on the anions in the VII column of the periodic table, and like chalcogenides, they can exhibit properties that make them excellent choices for radiation detectors. Figure 8 shows a number of spectra from the chalcogenide compounds developed for RTSD applications. Chalcohalides with the anion Cl are the lightest and feature the lowest stopping power of the class. Due to this, few Cl-based compounds are investigated as RTSD candidates. Additionally, due to the large bandgaps that form between heavy transition metal cations and the light anion Cl, many of the Cl-based chalcohalides that are investigated as radiation detectors are done so because they scintillate rather than directly ionize under radiation interactions. The compound β-$Hg_3S_2Cl_3$ has been developed the most as a gamma-ray detector out of the Cl anion compounds. The compound features good electronic properties with resistivity on the order of $10^{10}\,\Omega\,cm$, $(\mu\tau)_e$ of $10^{-4}\,cm^2/V$, and has demonstrated current mode responsivity to a pulsed x-ray beam.[63]

$CsPbBr_3$ is a Br-based semiconducting perovskite that can be produced through Bridgman growth or solution processing.[151] This compound has recently exhibited remarkable developmental breakthroughs, showing good $(\mu\tau)_e$ and $(\mu\tau)_h$ values and demonstrating gamma-ray spectra comparable to some of the best available RTSD materials.[64,150] He *et al.* recently demonstrated 3.8% resolution at 122 keV and 662 keV from a solution-grown $CsPbBr_3$ crystal.[150] The great electronic performance of this material along with its perovskite structure makes it an attractive candidate for both RTSD applications as well as organic-inorganic perovskite solar cells. The second of the Br-based chalcohalides, $Hg_3Se_2Br_2$, also exhibits attractive performance for RTSD applications. The congruently melting compound can be grown easily, has shown high resistivity and $(\mu\tau)_e$ values of $10^{11}\,\Omega\,cm$ and $10^{-4}\,cm^2/V$, respectively, and performed nearly as well as a CZT standard under incident radiation from a x-ray source.[65]

Several iodine-based chalcohalide compounds have also been explored for RTSD use. Examples of such materials include SbSeI; the Tl-based chalcohalides: Tl_4CdI_6, Tl_4HgI_6, Tl_6SI_4, Tl_6SeI_4, and $TlSn_2I_5$; the Hg-based chalcohalides: $Hg_3S_2I_2$, $Hg_3Se_2I_2$, and $Hg_3Te_2I_2$; and the defect perovskite chalcohalides $Rb_3Sb_2I_9$, $Rb_3Bi_2I_9$, $Cs_3Sb_2I_9$, and $Cs_3Bi_2I_9$. SbSeI features an interesting structure consisting of one-dimensional Sb-Se-I chains that zigzag along

Published under license by AIP Publishing.

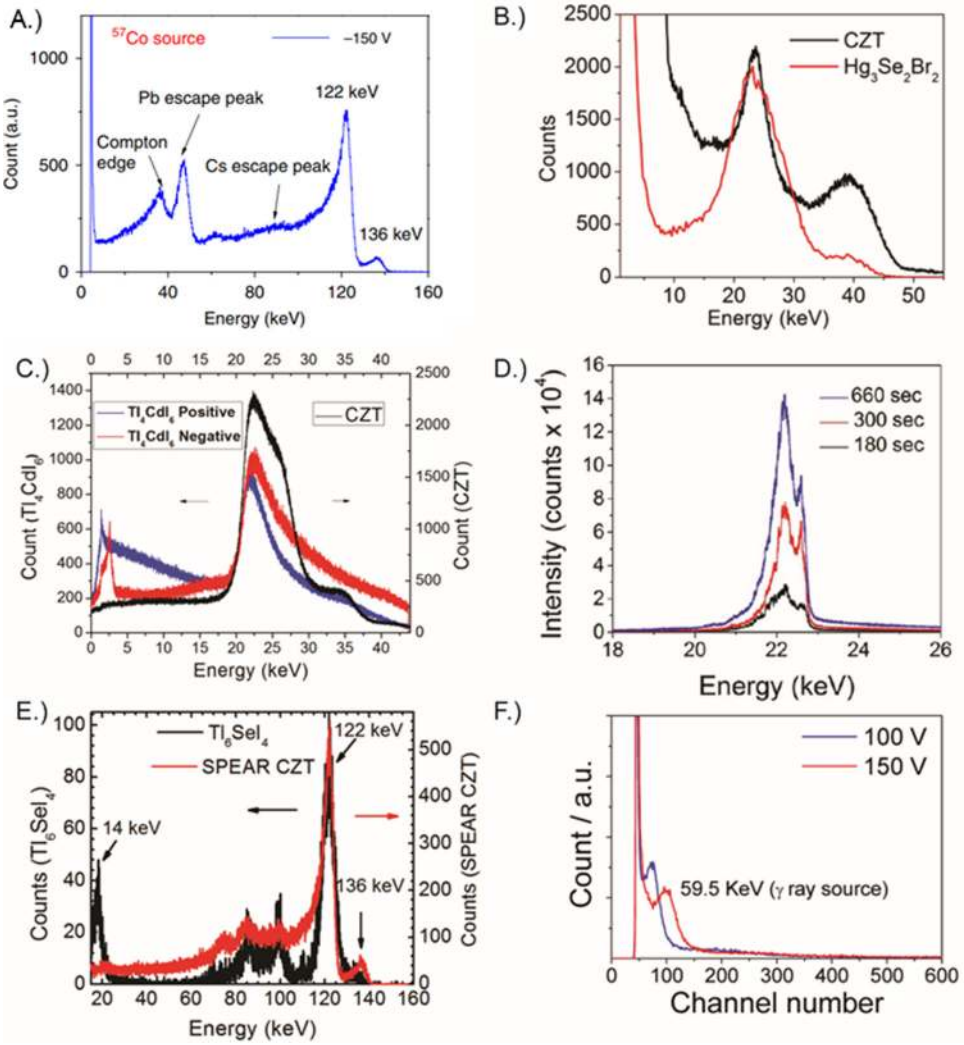

FIG. 8. Ag x-ray signals from the chalcohalides (a) $CsPbBr_3$ [Reprinted with permission from He *et al.*, Nat. Commun. **9**(1), 1609 (2018). Copyright 2018 He *et al.*, licensed under a Creative Commons Attribution License], (b) $Hg_3Se_2Br_2$ [Reprinted with permission from H. Li *et al.*, Cryst. Growth Des. **16**, 6446 (2016). Copyright 2016 American Chemical Society], (c) Tl_4CdI_6 [Reprinted with permission from Wang *et al.*, Cryst. Growth Des. **14**(5), 2401–2410 (2014). Copyright 2015 John Wiley and Sons], and (d) Tl_6SI_4 [Reprinted with permission from Nguyen *et al.*, Chem. Mater. **25**(14), 2868–2877 (2013). Copyright 2013 American Chemical Society]. (e) shows a ^{57}Co spectrum from Tl_6SeI_4 [Reprinted with permission from Johnsen *et al.*, J. Am. Chem. Soc. **133**(26), 10030–10033 (2011). Copyright 2011 American Chemical Society] and (f) shows ^{241}Am signals from a $Hg_3Se_2I_2$ detector [Reprinted with permission from He *et al.*, J. Am. Chem. Soc. **139**(23), 7939–7951 (2017). Copyright 2017 American Chemical Society].

the b-axis.[66] Similar ($\mu\tau$) product magnitudes for electrons and holes in SbSeI could make the compound capable of bipolar shaping and not need to rely on single polarity charge sensing techniques. Thus far, SbSeI has only shown current mode response to switched x-ray sources and has not yet been demonstrated to operate in pulse mode.

Tl_4CdI_6 is promising due to its high resistivity and its exceptional density and atomic number to provide high stopping power toward incident radiation. However, because it does not melt congruently, off-stoichiometric "red" and "black" phases can complicate the synthesis of the compound.[67] $TlCdI_6$ was additionally demonstrated to have similar ($\mu\tau$) product magnitudes and demonstrated near-identical x-ray spectra when collecting signals from electrons and holes.[67] Tl_4HgI_6 has similarly been reported to exhibit a good resistivity of 10^{11}–$10^{12}\,\Omega\,cm$ and ($\mu\tau$) values of $8\times10^{-4}\,cm^2/V$. Its exceptional physical and electronic properties have allowed for it to detect ^{137}Cs gamma rays with a resolution of 15%.[53] Perhaps the most attractive of these complex iodide compounds are the chalcohalides Tl_6SI_4 and Tl_6SeI_4, which are both P4/mnc structured crystals with atomic, physical, and electronic properties that already begin to rival that of CZT. Tl_6SI_4 is the compound with the highest effective-Z out of any potential RTSD candidate and has demonstrated $(\mu\tau)_e$ products above $10^{-3}\,cm^2/V$ and sensitivity to x-ray sources that outperformed that of a CZT standard.[68] While reportedly difficult to grow, Tl_6SeI_4 has demonstrated impressive $(\mu\tau)_e$ products near $10^{-2}\,cm^2/V$ and has reported gamma-ray spectra from a 122 keV ^{57}Co source with 4.7% resolution.[69] As seen in Fig. 8, the reported Tl_6SeI_4 spectra feature prominent escape x-rays peaks that can potentially add complexity to spectral fitting algorithms. Finally, the antiperovskite compound $TlSn_2I_5$ shows similar promising performance as a candidate RTSD compound.[70] $TlSn_2I_5$ has exhibited resistivity on the order of $10^{10}\,\Omega\,cm$ and $(\mu\tau)_e$ of $1.1\times10^{-3}\,cm^2/V$, and its low melting point of 315 °C makes growth and purification of the compound simpler

Published under license by AIP Publishing.

than many RTSD materials. While this compound has not exhibited spectroscopic gamma-ray spectra, attributed to the contrast in electron and hole ($\mu\tau$), it remains as a promising compound that is exempt from many of the thermodynamic challenges that plague perovskite-based RTSD compounds.

A number of compounds based on Hg as the cation are promising RTSD materials. The compounds $Hg_3S_2I_2$, $Hg_3Se_2I_2$, and $Hg_3Te_2I_2$ feature distinct crystal structures based on the noniodide anion that is incorporated into the compound. The high density and appropriate bandgaps exhibited by these compounds make them particularly attractive for RTSD devices. The work by He *et al.* investigated the growth and characterization of these antiperovskite-based compounds,[71] where the electronic property investigation showed resistivity on the order of 10^{11}–$10^{12}\,\Omega\,cm$ but relatively low $(\mu\tau)_e$ values of 10^{-6}–$10^{-5}\,cm^2/V$. $Hg_3Se_2I_2$ showed the best spectral performance of the three compounds and was able to weakly resolve the 59.5 keV photopeak from ^{241}Am. Finally, the defect perovskite compounds $Rb_3Sb_2I_9$, $Rb_3Bi_2I_9$, $Cs_3Sb_2I_9$, and $Cs_3Bi_2I_9$ have been investigated for RTSD applications. The materials currently produce $(\mu\tau)_e$ values on the order of 10^{-6}–$10^{-5}\,cm^2/V$ and have shown response to alpha particle radiation.[72] The heavy-Z chalcohalides are truly exciting compounds to watch develop for the future of high-performance RTSD sensors.

3. Other materials: Pnictogenides, oxides, carbides, and organic hybrid compounds

Apart from the exploration of semiconductors for use as room temperature detectors, several compounds do not fit in the categories above but have struck interest for their potential as RTSD sensor materials. These other materials can be categorized as pnictogenides, oxides, carbides, and organic hybrid compounds. Some of these materials are more electrically insulating than semiconducting but have still received interest for their feasibility as sensors that can directly collect charge. These compounds are typically desired to detect heavy charged particles in space, as solid-state neutron detectors, or to be used in accelerator instrumentation applications.

The first group of materials are pnictogenides, which are ionic compounds based on the anions P (Z = 15), As (Z = 33), and Sb (Z = 51). The compound $CdGeAs_2$ has received interest due to its carrier mobility on the order of $10^4\,cm^2/Vs$ and its unique ability to behave as a glass and form as an amorphous semiconductor.[73] Because it can detect radiation with a lack of crystallinity, this compound has unusual potential for a number of applications. Presently, however, the radiation response to $CdGeAs_2$ has been limited to current mode variations in DC currents.[73] Toward the development of solid-state neutron detectors, the compounds LiZnP and LiZnAs have shown potential due to their ability to incorporate the isotope ^6Li, which has a thermal neutron n,α cross section of over 900 b.[74] Montag *et al.* investigated the two compounds and their sensitivity to neutrons.[74] It was found that LiZnP showed some spectral response to neutrons emitting from a 200 kW reactor. The materials, however, were noted to exhibit a very wide range of resistivity (10^6 through $10^{11}\,\Omega\,cm$) and suffered from noise "bursts" that ruined signal collection. Through material quality improvement, it is likely that this promising compound can enhance its performance.

Relatively few oxides have a band structure that renders them as semiconducting instead of insulating. The compounds PbO and ZnO are examples with somewhat high gaps of 2.8 and 3.3 eV, respectively, and have thus been explored for use as RTSD materials. While PbO is a promising compound, it has seen relatively little development as a gamma detector. Willig reported in 1972 that single crystal PbO exhibited resistivity on the order of $10^{13}\,\Omega\,cm$, $(\mu\tau)_e$ products on the very low $10^{-8}\,cm^2/V$ scale, but responded to alpha particle bombardment with a spectrum.[80] Since then, there has been little interest in the compound; however, modern improvements to crystal growth could likely be employed to increase the $(\mu\tau)$ product in the material. Toward the development of ZnO, Zhao *et al.* grew high resistivity single crystals that were annealed as a treatment for donor ($V_O^{\bullet\bullet}$) and acceptor (V''_{Zn} and O''_i) traps.[152] The ZnO crystals demonstrated decent current mode performance under high intensity x-ray fields as well as pulsed electron beams. The crystal detection response was found to be remarkably fast, with a rise time of 3.3 ns when bombarded with electrons. The large bandgap of ZnO will likely limit its development to current mode applications such as dosimetry or x-ray instrumentation.

Carbides investigated for RTSD use are limited to SiC and diamond. With a large bandgap of 5.47 eV, diamond is a strong electrical insulator. Despite this, signals can be obtained by thin diamond detectors from strongly ionizing radiation such as alpha particles, protons, heavy ions, and intense x-ray beams. A review of diamond detectors by Adam *et al.* discusses the unique ways in which diamond differs from standard detectors.[153] Diamond has an extremely high resistivity of up to $10^{14}\,\Omega\,cm$, greater than any other compound explored here, and exhibits a $(\mu\tau)_e$ on the order of $10^{-8}\,cm^2/V$. The low $(\mu\tau)_e$ value underestimates the ability of diamond detectors to transport charge, as once carriers are in conduction bands they can obtain mobility over $1000\,cm^2/V\,s$.[153] Diamond as a detector has shown promise for use in high-energy charged particle and gamma ray detection facilities.[154,155] Unlike most RTSD compounds, which are intended for use as detectors in bulk form, diamond is typically utilized as a film deposited on a substrate through chemical vapor deposition.[156] Likewise, the 4-H polytype of SiC has seen some application as a solid-state detector material. SiC is particularly useful because its large bandgap renders it unexcitable from visible photons, which can simplify device design and greatly reduce the dark currents from the detector under bias. The section of the SiC review by Wright and Horsfall on radiation detection capability presents a summary on the processing of SiC for sensor application, as well as the status of past efforts to develop the material.[157] Notably, SiC has been able to produce gamma-ray response to alpha and beta particles, as well as the 5.8 keV x-rays of ^{55}Fe with a resolution of around 1 keV.[158]

Perhaps the most exotic group of potential RTSD materials is organic semiconducting compounds. Organic-inorganic hybrid perovskites have recently gained attention from their impressive performance as photovoltaics and have strong potential to serve as radiation sensors. Several groups have now shown the potential of using single crystals of perovskite compounds based on methylammonium (MA) and formamidinium (FA) lead iodide and bromide as solid-state organic radiation detectors.[82,84,86,89,159,160] The hybrid organic-inorganic compounds are particularly interesting

Published under license by AIP Publishing.

for RTSD sensors due to their ability to be cheaply grown from solution at relatively low temperatures below 150 °C. The mobility-lifetime products in hybrid organic single crystals have been shown to exceed 10^{-2} cm^2/V. Several compounds, highlighted in Fig. 9, have demonstrated remarkable performance toward detection gamma rays.

$MAPbI_3$ development within the last few years has culminated in several compounds that have produced promising responses to radiation in both pulse and current mode applications. He *et al.* have demonstrated $MAPbI_3$ spectra from a variety of gamma-emitting sources, with 6.8% resolution demonstrated at 122.[84] $MAPbBr_3$ compensated with Cl to reduce noise and leakage currents has demonstrated equally impressive spectra, including 6.5% resolution at 662 keV.[89] Both of these MA-based compounds exhibit ($\mu\tau$) products on the order of 10^{-3} cm^2/V, which compares to the performance of commercial grade CZT. Single crystals of $FAPbI_3$, compensated with Cs and Br anion and cation dopants, have demonstrated some of the highest ($\mu\tau$) of any emerging RTSD material, on the order of 10^{-1} cm^2/V.[86] Additionally, both of these materials are grown from solutions, in glass beakers/vials, with crystallization occurring over the course of several hours to days.[84,86,89]

Nonperovskite organic crystals have demonstrated potential for good performance following simple growth from solution. Single crystals of rubrene have recently demonstrated nonspectroscopic response to ^{252}Cf alpha particle sources.[161] Organic-inorganic hybrid perovskites and other organic semiconductors have much promise for RTSD use; however, due to low thermodynamic stabilities, they often breakdown under moderate field conditions and are only stable for a few months.[82]

IV. PERSPECTIVES AND CONCLUSION

The development of RTSD compounds is pursued toward the goal of developing sensitive radiation detectors that can alert, identify, and characterize radiation. Current industry standard detection systems based on NaI:Tl can detect and/or identify isotopes down to gamma-ray fluxes between 1 and 0.1 γ/cm^2 s in a span of 1 or 2 min of measurement time. Advantages gained by the development of RTSD compounds are not simply incremental; the better signal-to-noise gained by semiconductor energy conversion and signal generation mechanisms can allow for order of magnitude improvements. The ramifications of developing an ideal RTSD sensor and integrating it into radiation detection systems could have significant impacts on global nuclear security.

A. Promising materials to drive innovation

With such a large number of compounds in contention for use in RTSD applications, it is interesting and useful to compare the characteristics of each material. One method of accomplishing this is to select a key physical and electronic property to represent the performance of each compound. The most important physical quality is the electron density of a material, as determines the efficiency of a compound at interacting with high-energy photons. For electronic performance, the ($\mu\tau$) product is of most importance because it determines the charge collection efficiency and minimum operating bias of a detector. Because most compounds feature a $(\mu\tau)_e$ that exceeds $(\mu\tau)_h$, the electron mobility-lifetime product is perhaps the most important electronic property an RTSD compound possesses. Figure 10 amasses each of the compounds

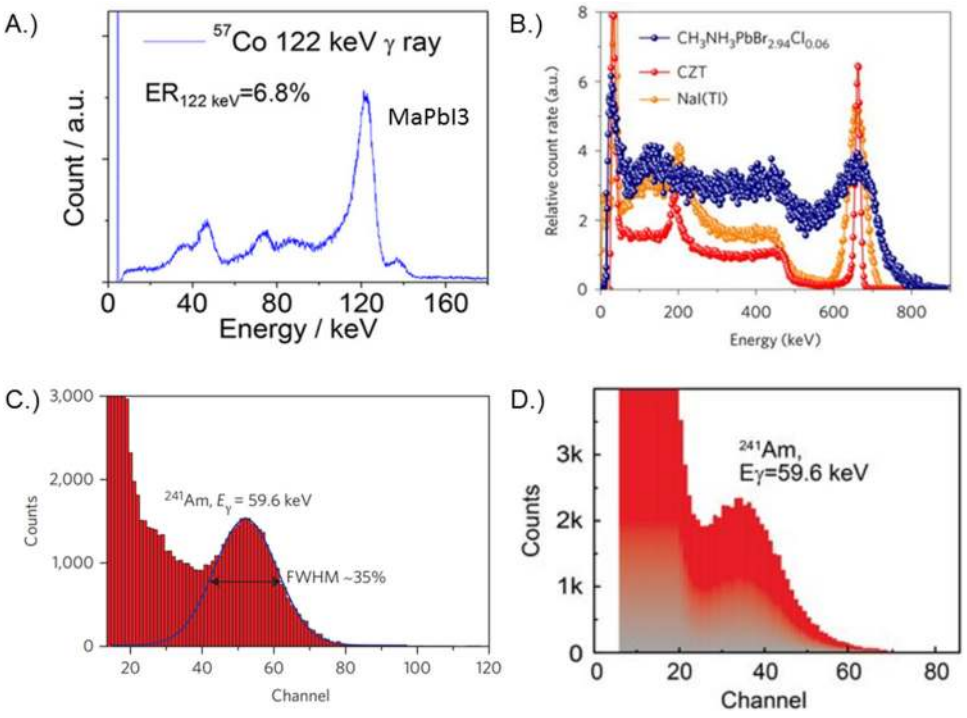

FIG. 9. (a) A 6.8% resolution photopeak from the 122 keV emission of ^{57}Co. Reprinted with permission from He *et al.*, ACS Photonics **5**(10), 4132–4138 (2018). Copyright 2018 American Chemical Society. (b) A $MAPbBr_3$:Cl spectra showing 6.5% resolution for the 662 keV emission of ^{137}Cs. Reprinted with permission from Wei *et al.*, Nat. Mater. **16**(8), 826 (2017). Copyright 2017 Springer Nature. (c) $FAPbI_3$ response to the 59 keV emission of ^{241}Am. Reprinted with permission from Yakunin *et al.*, Nat. Photonics **10**, 585 (2016). Copyright 2016 Springer Nature. (d) $CsFAPbI_3$:Br response to the 59 keV emission of ^{241}Am. Reprinted with permission from Nazarenko *et al.*, NPG Asia Mater. **9**, e373 (2017). Copyright Nazarenko *et al.*, licensed under a Creative Commons Attribution Licence.

Published under license by AIP Publishing.

discussed in this review, with the x-axis listing the electron density for each compound and the y-axis listing the $(\mu\tau)_e$ reported for each material in Table 1. It should be understood that the set of data collected in Fig. 10 was collected under a variety of sample thicknesses and testing conditions. One-to-one $(\mu\tau)_e$ comparisons between different compounds do not provide a realistic comparison between materials. As an example, HgI_2 falls among the middle of the pack in electronic and physical properties, yet is presently among the best compounds at producing high-resolution room temperature gamma-ray spectra. On an individual basis, however, the level of electronic and physical promise shown by various compounds can be assessed.

Some standout materials in Fig. 10 include CdTe, CZT, CdMnTe, CdTeSe, TlBr, $MAPbBr_3$, $MAPbI_3$, Tl_6SeI_4, and $TlInSe_2$ that exhibit the best combination of $(\mu\tau)_e$ values and electron density of all the compiled RTSD materials. This fact emphasizes the importance that processing and defect control has on the spectral performance of an RTSD compound.

Perhaps the most interesting materials emerging from the field of RTSD development are the hybrid organic perovskites. The astounding charge transport in these compounds stems from the band structure of inorganic sublattices enabling rapid mobility while the CH_3NH_3 sublattice screens out electron-hole attraction to minimize recombination.[163] High electron density created by a high charge-to-mass ratio make them much more efficient at stopping gamma rays than most high-Z inorganic compounds. Perhaps the most disruptive aspect of hybrid perovskites is their synthesis routes. Although most RTSD compounds are grown from melt-based methods in high temperature furnaces over periods up to the scale of weeks, the organic-inorganic perovskites are capable of being grown from solution in glassware at near-ambient temperatures. Yield, output rate, and cost per volume of these compounds make them compelling to further investigate for applications as large volume detectors. If electronic stability can be improved in these compounds, hybrid organic perovskites could possibly lead the field of RTSD research toward more effective radiation detectors in upcoming years.

Many of the fundamental issues faced by emerging RTSD candidates are the same challenges that CdTe, CZT, TlBr, and HgI_2 have faced for decades. Poor hole mobility, secondary phases, and defects require single polarity charge sensing and 2D/3D depth correction to be applied to get the best resolution from a sensor. A more severe issue is the polarization phenomena that are often present in emerging RTSD compounds and are nontrivial to correct. Unfortunately, the material aspects that make compounds attractive for gamma ray detection also make them particularly

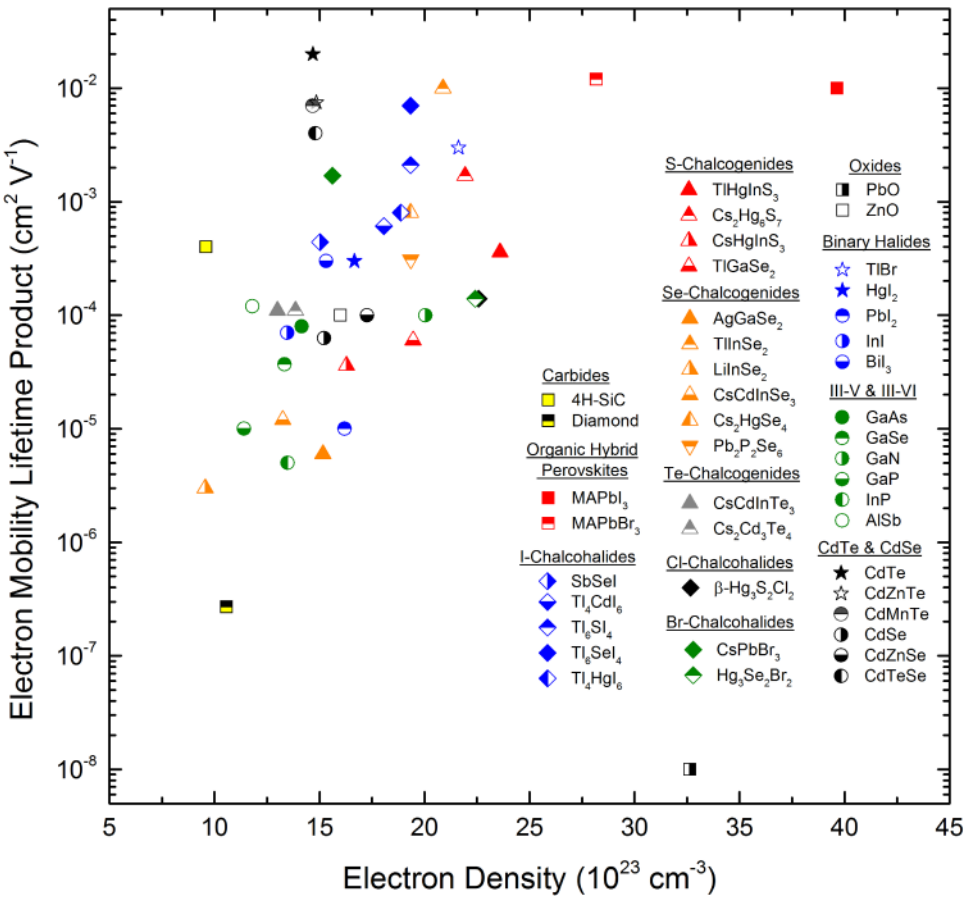

FIG. 10. A comparison of the electronic and physical properties reported for the wide number of compounds investigated as RTSD materials. Electron density computed by the methods from Manohara *et al.*[162]

Published under license by AIP Publishing.

susceptible to polarization. RTSD semiconductors are designed to feature high atomic number atoms bound into a lattice that exhibits a bandgap between ~1.5 and 2.5 eV. The strong ionic bonding nature between heavy metal cations and group VI and VIII anions that creates appropriate bandgaps in these semiconductors also imparts soft lattices and high ionic conductivity. The mobility of ionic species in these compounds makes their lattices receptive to vacancies and antisite defects, which lead to defects complexes that polarize detectors under extended time under bias.[164] Practical challenges such as toxicity are also important to consider, as many of the candidate RTSD compounds are based on elements and compounds that are toxic and require excessive protective equipment while manufacturing.

Great radiation detection performance often comes at a high production cost. In most cases, RTSD constituent materials have to be refined, purified, grown at slow rates in high temperature furnaces, and mechanically processed into detectors in order to produce spectrometer quality sensors. This can make RTSD technologies more expensive than competing scintillation detectors such as NaI:Tl. Several emerging chalcogenides, chalcohalides, and binary iodide compounds melt congruently at low temperatures, which reduces the complexity and cost associated with purification and growth. Focused development on solution-based growth techniques that can produce semiconducting materials with properties sufficient for RTSD application can further drive down the cost associated with sensor production. Inorganic perovskites such as $CsPbBr_3$, hybrid organic perovskites, and organic semiconducting crystals can be grown in solution at relatively low cost. For instance, hybrid perovskite single crystals can be grown from solution and need only be moderately pure to produce spectrometer quality material at the referenced cost of \$0.5–\$1/cm^{-3}.[82]

B. Perspectives on technology improvements from RTSDs

Displacing established technology can be a challenge for emerging technologies. Many categories of radiation detection technologies, particularly those with nuclear security applications, would benefit greatly from the resolution gains brought by RTSDs. RTSD spectrometers can bring improvements to the field by replacing or integrating into existing systems in one of two manners:

1. providing equal identification capability at smaller volumes as lower resolution spectroscopic detectors or
2. enabling higher identification capability at equivalent volumes as lower resolution spectroscopic detectors.

Due to the limitations on crystal growth volume and yield discussed in this work, the most direct beneficiaries from advancements in RTSDs will be detection systems requiring small to moderately sized (several cubic millimeter to cubic centimeter volume) sensors. Personal radiation detectors (PRDs), which are limited to small size and mass by consensus standards,[165] must ideally produce the highest signal-to-noise in the smallest sizes possible. The combination of high efficiency and resolution within compact crystal volumes enables RTSDs to be among the best options for advancing PRD sensor technology. Particularly, higher resolution in compact detection instruments can allow detectors to have higher selectivity at identifying radionuclides in an environment while additionally discriminating against background or naturally occurring radioactive materials (NORM). Several manufacturers have recently integrated CZT into PRDs that are now commercial off-the-shelf (COTs) equipment, and further development into RTSD sensors that are of lower cost, higher yield, and have better charge transport will continue to improve the detection limits in PRD systems.

Radioisotope identification devices (RIDs) are also among the most obvious beneficiaries of improved RTSDs. While several manufacturers currently produce CZT-based RIDs that meet or exceed industry consensus standards, the field of COTs handheld RIDs predominantly consists of NaI(Tl) sensors. Energy resolution is a key factor that drives false alarm rate and identification capabilities in handheld spectrometers.[166] Therefore, implementing higher resolution RTSD sensors into the field of handheld RIDs could enable detectors to produce accurate identifications at longer standoff distances and shorter measurement times than comparably sized NaI(Tl) sensors. Methods used in semiconductor detectors to isolate interaction positions in 3D can also be used to enable localization and threat isolation capabilities in RID systems.[167] Similarly, many other categories of detection systems can benefit from the enhanced minimum signal to noise ratio when scintillator logs are replaced with single crystals or arrays of RTSD sensors. Backpack-based systems, area spectrometers, or the emerging field of wearable radiation sensors (i.e., spectrometers built into clothing) would additionally benefit from compact, high-resolution RTSDs.

Radiation detection systems that require larger detection volumes may always remain a niche that is better filled by scintillators. For instance, it is difficult to imagine feasible radiation portal monitors comprised of large semiconductor sensors or arrays of smaller crystals. Applications where maximum detection efficiency is required to benefit more from larger sized scintillators than higher resolution RTSD sensors. Nonetheless, a number of practical applications remain where large sized HPGe crystals could be replaced with more fieldable RTSD-based systems where spectral features are more important than absolute detection efficiency. Reducing weight and the power draw by HPGe spectrometers could lead to air, mobile, and remote-lab systems where RTSD crystals manufactured in large volumes would be more practical than HPGe systems running on sterling coolers or liquid nitrogen refrigerant.

C. Conclusion and future

In conclusion, room temperature semiconductor detectors are a critical tool for applications where it is necessary to detect the presence of radioactive materials. Despite the robust criteria that must be satisfied for semiconducting compounds to serve as gamma-ray sensors, a number of emerging compounds feature strong potential to perform in the role. However, for RTSD compounds to displace NaI(Tl) in commercial devices, the key factor that must be improved upon is cost. Future development efforts in the field should drive toward RTSDs that are produced from precursor materials and synthesis routes that are of lower cost. Ideal RTSDs should be capable of being produced in higher yields than

Published under license by AIP Publishing.

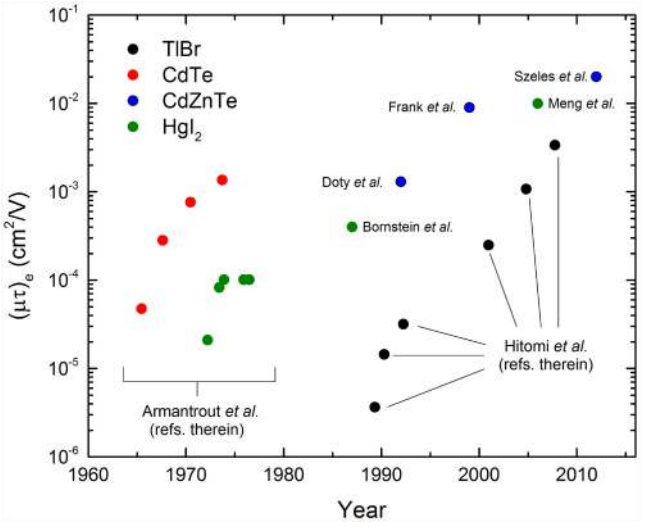

FIG. 11. The best $(\mu\tau)_e$ products as a function of the year reported for the materials CdTe, CdZnTe, HgI_2, and TlBr. Selected value references are taken from Armantrout *et al.*,[168] Bornstein and Bube,[169] Doty *et al.*,[170] Franc *et al.*,[171] Szeles,[172] and Hitomi *et al.*[173]

what are seen from predominant semiconductor detector technologies such as CZT and HPGe. In perspective, the most attractive emerging materials to achieve this goal appear to be inorganic and hybrid organic-inorganic perovskite compounds that have emerged in development over the past few years.

As a final note, it should be emphasized that the properties exhibited by these promising semiconducting materials indicate only how good the materials are in their present stage of development. Strong skepticism or optimism toward materials based on their initially reported properties is a dangerous tendency. As a material progresses in development and becomes better understood, crystals with larger volumes and lower concentrations of defects are able to provide better performance as gamma-ray sensors. Because of this, it can be perilous to the field of RTSD materials to ignore promising materials because first studies on their properties did not yield tremendous promise. To emphasize this, Fig. 11 shows the best-reported $(\mu\tau)_e$ values for TlBr, CdTe, and CZT with the year that the data were reported. While techniques for measuring electronic properties have increased through time, the trajectory of property improvement with increasing development can be seen for each of the top-contending RTSD materials. If TlBr, for instance, was not examined further after its initial study in 1989 due to poor electron mobility, it would not be one of the forefront RTSD materials today.

ACKNOWLEDGMENTS

The authors declare no competing financial interests. This research did not receive any specific grant from funding agencies in the public, commercial, or not-for-profit sectors. Pacific Northwest National Laboratory release PNNL-SA-129696.

REFERENCES

[1]B. Obama, *National Security Strategy of the United States* (DIANE Publishing, 2010).
[2]D. J. Trump, *National Security Strategy of the United States of America* (Executive Office of the President, Washington, DC, 2017).
[3]B. Obama, *National Strategy for Counterterrorism* (US White House, 2011), Vol. 28, p. 201.
[4]B. D. Milbrath *et al.*, "Radiation detector materials: An overview," J. Mater. Res. **23**(10), 2561–2581 (2008).
[5]G. F. Knoll, *Radiation Detection and Measurement* (John Wiley & Sons, 2010).
[6]ORTEC, *GEM Series Coaxial HPGe Detector Product Configuration Guide* (AM Technology, 2009).
[7]A. Owens, *Compound Semiconductor Radiation Detectors* (Taylor & Francis, 2012).
[8]K. Hecht, "Zum Mechanismus des lichtelektrischen Primärstromes in isolierenden Kristallen," Z. Phys. **77**(3), 235–245 (1932).
[9]H. H. Barrett, J. D. Eskin, and H. B. Barber, "Charge transport in arrays of semiconductor gamma-ray detectors," Phys. Rev. Lett. **75**(1), 156–159 (1995).
[10]W. J. McNeil *et al.*, "Single-charge-carrier-type sensing with an insulated Frisch ring CdZnTe semiconductor radiation detector," Appl. Phys. Lett. **84**(11), 1988–1990 (2004).
[11]D. S. McGregor and H. Hermon, Nucl. Instrum. Methods Phys. Res. A **395**, 101 (1997).
[12]A. Owens and A. Peacock, "Compound semiconductor radiation detectors," Nucl. Instrum. Methods Phys. Res. A **531**(1), 18–37 (2004).
[13]P. N. Luke and M. Amman, "Room-temperature replacement for Ge detectors—Are we there yet?," IEEE Trans. Nucl. Sci. **54**(4), 834–842 (2007).
[14]P. J. Sellin and J. Vaitkus, "New materials for radiation hard semiconductor detectors," Nucl. Instrum. Methods Phys. Res. A **557**(2), 479–489 (2006).
[15]V. M. Zaletin and V. P. Varvaritsa, "Wide-bandgap compound semiconductors for x- or gamma-ray detectors," Russ. Microelectron. **40**(8), 543–552 (2011).
[16]S. Awadalla, *Solid-State Radiation Detectors Technology and Applications* (CRC Press, 2015).
[17]K. Iniewski, *Semiconductor Radiation Detection Systems* (CRC Press, 2010).
[18]T. Takahashi and S. Watanabe, "Recent progress in CdTe and CdZnTe detectors," IEEE Trans. Nucl. Sci. **48**(4), 950–959 (2001).
[19]M. Amman *et al.*, "Evaluation of THM-grown CdZnTe material for large-volume gamma-ray detector applications," IEEE Trans. Nucl. Sci. **56**(3), 795–799 (2009).
[20]C. Szeles *et al.*, "Fabrication of high performance CdZnTe quasi-hemispherical gamma-ray CAPture™ plus detectors," Proc. SPIE **6319**, 631909 (2006).
[21]C. Szeles *et al.*, "Development of the high-pressure electro-dynamic gradient crystal-growth technology for semi-insulating CdZnTe growth for radiation detector applications," J. Electron. Mater. **33**(6), 742–751 (2004).
[22]K. Hitomi *et al.*, "Recent development of TlBr gamma-ray detectors," IEEE Trans. Nucl. Sci. **58**(4), 1987–1991 (2011).
[23]H. Kim *et al.*, "Developing larger TlBr detectors—Detector performance," IEEE Trans. Nucl. Sci. **56**(3), 819–823 (2009).
[24]W. Wu *et al.*, "Traveling heater method growth and characterization of CdMnTe crystals for radiation detectors," Phys. Status Solidi C **13**, 408 (2016).
[25]Y. Cui, A. Bolotnikov, A. Hossain, G. Camarda, A. Mycielski, G. Yang, D. Kochanowskab, M. Witkowska-Baran, and R. James, "CdMnTe in x-ray and gamma-ray detection: Potential applications", Report No. BNL-81493-2008-CP, Brookhaven National Laboratory, Upton, New York, USA, 2008.
[26]R. Rafiei *et al.*, "High-purity CdMnTe radiation detectors: A high-resolution spectroscopic evaluation," IEEE Trans. Nucl. Sci. **60**(2), 1450–1456 (2013).
[27]K. H. Kim *et al.*, "Spectroscopic properties of large-volume virtual Frisch-grid CdMnTe detectors," J. Korean Phys. Soc. **66**(11), 1761–1765 (2015).
[28]A. Burger, I. Shilo, and M. Schieber, "Cadmium selenide: A promising novel room temperature radiation detector," IEEE Trans. Nucl. Sci. **30**(1), 368–370 (1983).
[29]M. Roth, "Advantages and limitations of cadmium selenide room temperature gamma ray detectors," Nucl. Instrum. Methods Phys. Res. A **283**(2), 291–298 (1989).
[30]V. Kishore *et al.*, "Structural and electrical measurements of CdZnSe composite," Bull. Mater. Sci. **28**(5), 431–436 (2005).

Published under license by AIP Publishing.

[31]U. N. Roy *et al.*, "Growth of $CdTexSe_{1-x}$ from a Te-rich solution for applications in radiation detection," J. Cryst. Growth **386**, 43–46 (2014).
[32]U. Roy *et al.*, "Growth and characterization of CdTeSe for room-temperature radiation detector applications," Proc. SPIE **8852**, 885210 (2013).
[33]S. M. Sze and K. K. Ng, *Physics of Semiconductor Devices* (John Wiley & Sons, 2006).
[34]B.-C. Juang *et al.*, "Characterization of GaSb photodiode for gamma-ray detection," Appl. Phys. Express **9**(8), 086401 (2016).
[35]R. C. Alig and S. Bloom, Phys. Rev. Lett. **35**, 1522 (1975).
[36]H. Nakatani *et al.*, "GaSe nuclear particle detectors," Nucl. Instrum. Methods Phys. Res. A **283**(2), 303–309 (1989).
[37]K. C. Mandal *et al.*, "GaSe and GaTe anisotropic layered semiconductors for radiation detectors," Proc. SPIE **6706**, 67060E (2007).
[38]K. Zdansky *et al.*, "Evaluation of semiinsulating annealed InP:Ta for radiation detectors," IEEE Trans. Nucl. Sci. **53**(6), 3956–3961 (2006).
[39]J. H. Yee, S. P. Swierkowski, and J. W. Sherohman, "ALSB as a high-energy photon detector," IEEE Trans. Nucl. Sci. **24**(4), 1962–1967 (1977).
[40]H. Li *et al.*, "$TlHgInS_3$: An indirect-band-gap semiconductor with x-ray photoconductivity response," Chem. Mater. **27**(15), 5417–5424 (2015).
[41]H. Li *et al.*, "Crystal growth and characterization of the x-ray and γ-ray detector material $Cs_2Hg_6S_7$," Cryst. Growth Des. **12**(6), 3250–3256 (2012).
[42]H. Li *et al.*, "Investigation of semi-insulating $Cs_2Hg_6S_7$ and Cs_2Hg_6-xCd*x*S_7 alloy for hard radiation detection," Cryst. Growth Des. **14**(11), 5949–5956 (2014).
[43]H. Li *et al.*, "$CsHgInS_3$: A new quaternary semiconductor for γ-ray detection," Chem. Mater. **24**(22), 4434–4441 (2012).
[44]S. Johnsen *et al.*, "Thallium chalcogenide-based wide-band-gap semiconductors: $TlGaSe_2$ for radiation detectors," Chem. Mater. **23**(12), 3120–3128 (2011).
[45]U. N. Roy *et al.*, "Crystal growth, characterization, and fabrication of $AgGaSe_2$ crystals as novel material for room-temperature radiation detectors," Proc. SPIE **5540**, 177–180 (2004).
[46]I. V. Alekseev, "A neutron semiconductor detector based on $TlInSe_2$," Instrum. Exp. Tech. **51**(3), 331–335 (2008).
[47]D. G. Kilday *et al.*, "Electronic structure of the 'chain' chalcogenide $TlInSe_2$," Phys. Rev. B **35**(2), 660–663 (1987).
[48]I. Alekseev, Inorganic Materials **28**, 1961–1964 (1993).
[49]E. Tupitsyn *et al.*, "Single crystal of $LiInSe_2$ semiconductor for neutron detector," Appl. Phys. Lett. **101**(20), 202101 (2012).
[50]Z. W. Bell *et al.*, "Neutron detection with $LiInSe_2$," Proc. SPIE **9593**, 95930D (2015).
[51]A. C. Stowe *et al.*, "Crystal growth in $LiGaSe_2$ for semiconductor radiation detection applications," J. Cryst. Growth **379**, 111–114 (2013).
[52]H. Li *et al.*, "$CsCdInQ_3$ (Q = Se, Te): New photoconductive compounds as potential materials for hard radiation detection," Chem. Mater. **25**(10), 2089–2099 (2013).
[53]D. Kahler *et al.*, "Performance of novel materials for radiation detection: Tl_3AsSe_3, $TlGaSe_2$, and Tl_4HgI_6," Nucl. Instrum. Methods Phys. Res. A **652**(1), 183–185 (2011).
[54]J. Androulakis *et al.*, "Dimensional reduction: A design tool for new radiation detection materials," Adv. Mater. **23**(36), 4163–4167 (2011).
[55]P. L. Wang *et al.*, "Hard radiation detection from the selenophosphate $Pb_2P_2Se_6$," Adv. Funct. Mater. **25**(30), 4874–4881 (2015).
[56]P. L. Wang *et al.*, "Refined synthesis and crystal growth of $Pb_2P_2Se_6$ for hard radiation detectors," Cryst. Growth Des. **16**, 5100 (2016).
[57]W. Lin *et al.*, "$Cu_2I_2Se_6$: A metal–inorganic framework wide-bandgap semiconductor for photon detection at room temperature," J. Am. Chem. Soc. **140**(5), 1894–1899 (2018).
[58]M. R. Squillante *et al.*, "InI nuclear radiation detectors," in *IEEE Conference on Nuclear Science Symposium and Medical Imaging Conference, Orlando, FL, 25–31 October 1992* (IEEE, 1992).
[59]T. Onodera, K. Hitomi, and T. Shoji, "Fabrication of indium iodide x- and gamma-ray detectors," IEEE Trans. Nucl. Sci. **53**(5), 3055–3059 (2006).
[60]T. Onodera, K. Baba, and K. Hitomi, *Evaluation of Antimony Tri-Iodide Crystals for Radiation Detectors* (Science and Technology of Nuclear Installations, 2018).
[61]N. J. Podraza *et al.*, "Band gap and structure of single crystal BiI_3: Resolving discrepancies in literature," J. Appl. Phys. **114**(3), 033110 (2013).
[62]T. Saito *et al.*, "BiI_3 single crystal for room-temperature gamma ray detectors," Nucl. Instrum. Methods Phys. Res. A **806**, 395–400 (2016).
[63]A. C. Wibowo *et al.*, "An unusual crystal growth method of the chalcohalide semiconductor, β-$Hg_3S_2Cl_2$: A new candidate for hard radiation detection," Cryst. Growth Des. **16**, 2678 (2016).
[64]C. C. Stoumpos *et al.*, "Crystal growth of the perovskite semiconductor $CsPbBr_3$: A new material for high-energy radiation detection," Cryst. Growth Des. **13**(7), 2722–2727 (2013).
[65]H. Li *et al.*, "Mercury chalcohalide semiconductor $Hg_3Se_2Br_2$ for hard radiation detection," Cryst. Growth Des. **16**, 6446 (2016).
[66]A. C. Wibowo *et al.*, "Photoconductivity in the chalcohalide semiconductor, SbSeI: A new candidate for hard radiation detection," Inorg. Chem. **52**(12), 7045–7050 (2013).
[67]S. Wang *et al.*, "Crystal growth of Tl_4CdI_6: A wide band gap semiconductor for hard radiation detection," Cryst. Growth Des. **14**(5), 2401–2410 (2014).
[68]S. L. Nguyen *et al.*, "Photoconductivity in Tl_6SI_4: A novel semiconductor for hard radiation detection," Chem. Mater. **25**(14), 2868–2877 (2013).
[69]S. Johnsen *et al.*, "Thallium chalcohalides for x-ray and γ-ray detection," J. Am. Chem. Soc. **133**(26), 10030–10033 (2011).
[70]W. Lin *et al.*, "$TlSn_2I_5$, a robust halide antiperovskite semiconductor for γ-ray detection at room temperature," ACS Photonics **4**, 1805 (2017).
[71]Y. He *et al.*, "Defect antiperovskite compounds $Hg_3Q_2I_2$ (Q = S, Se, and Te) for room-temperature hard radiation detection," J. Am. Chem. Soc. **139**(23), 7939–7951 (2017).
[72]K. M. McCall *et al.*, "α-particle detection and charge transport characteristics in the $A_3M_2I_9$ defect perovskites (A = Cs, Rb; M = Bi, Sb)," ACS Photonics **5**(9), 3748–3762 (2018).
[73]B. R. Johnson *et al.*, FY07 Annual Report: Amorphous Semiconductors for Gamma Radiation Detection (ASGRAD) (Pacific Northwest National Laboratory, 2008).
[74]B. W. Montag *et al.*, "Device fabrication, characterization, and thermal neutron detection response of LiZnP and LiZnAs semiconductor devices," Nucl. Instrum. Methods Phys. Res. A **836**, 30–36 (2016).
[75]K. Kuriyama, T. Kato, and K. Kawada, "Optical band gap of the filled tetrahedral semiconductor LiZnAs," Phys. Rev. B **49**(16), 11452–11455 (1994).
[76]K. Kuriyama and T. Katoh, "Optical band gap of the filled tetrahedral semiconductor LiZnP," Phys. Rev. B **37**(12), 7140 (1988).
[77]F. Nava *et al.*, "Silicon carbide and its use as a radiation detector material," Meas. Sci. Technol. **19**(10), 102001 (2008).
[78]M. Friedl, *Diamond Detectors for Ionizing Radiation* (Austrian Academy of Sciences, 1999).
[79]G. Conte *et al.*, "Temporal response of CVD diamond detectors to modulated low energy x-ray beams," Phys. Status Solidi A **201**(2), 249–252 (2004).
[80]W. R. Willig, "Large bandgap mercury and lead compounds for nuclear particle detection," Nucl. Instrum. Methods **101**(1), 23–24 (1972).
[81]X. Zhao, L. Chen, Y. He, J. Liu, W. Peng, Z. Huang, X. Qi, Z. Pan, W. Zhang, Z. Zhang, and X. Ouyang, Appl. Phys. Lett. **108**, 171103 (2016).
[82]S. Yakunin *et al.*, "Detection of gamma photons using solution-grown single crystals of hybrid lead halide perovskites," Nat. Photonics **10**, 585 (2016).
[83]X. Mettan *et al.*, "Tuning of the thermoelectric figure of merit of $CH_3NH_3MI_3$ (M = Pb, Sn) photovoltaic perovskites," J. Phys. Chem. C **119**(21), 11506–11510 (2015).
[84]Y. He *et al.*, "Resolving the energy of γ-ray photons with $MAPbI_3$ single crystals," ACS Photonics **5**(10), 4132–4138 (2018).
[85]Q. Han *et al.*, "Single crystal formamidinium lead iodide ($FAPbI_3$): Insight into the structural, optical, and electrical properties," Adv. Mater. **28**, 2253 (2016).
[86]O. Nazarenko *et al.*, "Single crystals of caesium formamidinium lead halide perovskites: Solution growth and gamma dosimetry," NPG Asia Mater. **9**, e373 (2017).
[87]H. Wei *et al.*, "Sensitive x-ray detectors made of methylammonium lead tribromide perovskite single crystals," Nat. Photonics **10**(5), 333–339 (2016).

Published under license by AIP Publishing.

[88]S. Ryu *et al.*, "Voltage output of efficient perovskite solar cells with high open-circuit voltage and fill factor," Energy Environ. Sci. **7**(8), 2614–2618 (2014).
[89]H. Wei *et al.*, "Dopant compensation in alloyed CH_3 NH_3 $PbBr_{3-x}Cl_x$ perovskite single crystals for gamma-ray spectroscopy," Nat. Mater. **16**(8), 826 (2017).
[90]J. F. Butler, C. L. Lingren, and F. P. Doty, "$Cd_{1-x}Zn_xTe$ gamma ray detectors," IEEE Trans. Nucl. Sci. **39**(4), 605–609 (1992).
[91]S. Del Sordo *et al.*, "Progress in the development of CdTe and CdZnTe semiconductor radiation detectors for astrophysical and medical applications," Sensors **9**(5), 3491–3526 (2009).
[92]Q. Zhang *et al.*, "Progress in the development of CdZnTe unipolar detectors for different anode geometries and data corrections," Sensors **13**(2), 2447–2474 (2013).
[93]A. E. Bolotnikov *et al.*, "Use of high-granularity CdZnTe pixelated detectors to correct response non-uniformities caused by defects in crystals," Nucl. Instrum. Methods Phys. Res. A **805**, 41–54 (2016).
[94]M. Streicher *et al.*, "A portable 2 × 2 digital 3D CZT imaging spectrometer system," in *2014 IEEE Nuclear Science Symposium and Medical Imaging Conference (NSS/MIC), Seattle, WA, 8–15 November 2014* (IEEE, 2014).
[95]K. Iniewski, "CZT detector technology for medical imaging," J. Instrum. **9**(11), C11001 (2014).
[96]C. Scheiber and J. Chambron, "Cdte detectors in medicine: A review of current applications and future perspectives," Nucl. Instrum. Methods Phys. Res. A **322**(3), 604–614 (1992).
[97]Y. Eisen and A. Shor, "CdTe and CdZnTe materials for room-temperature x-ray and gamma ray detectors," J. Cryst. Growth **184–185**, 1302–1312 (1998).
[98]R. Triboulet and P. Siffert, *CdTe and Related Compounds; Physics, Defects, Hetero- and Nano-Structures, Crystal Growth, Surfaces and Applications Physics, CdTe-Based Nanostructures, CdTe-Based Semimagnetic Semiconductors, Defects* (Elsevier Science, 2009).
[99]P. Rudolph, "Non-stoichiometry related defects at the melt growth of semiconductor compound crystals—A review," Cryst. Res. Technol. **38**(78), 542–554 (2003).
[100]C. H. Henager *et al.*, *Property Improvement in CZT via Modeling and Processing Innovations. Te-Particles in Vertical Gradient Freeze CZT: Size and Spatial Distributions and Constitutional Supercooling* (Pacific Northwest National Lab, PNNL, Richland, WA, 2014).
[101]A. E. Bolotnikov *et al.*, "Extended defects in CdZnTe radiation detectors," IEEE Trans. Nucl. Sci. **56**(4), 1775–1783 (2009).
[102]C. Candelise, M. Winskel, and R. Gross, "Implications for CdTe and CIGS technologies production costs of indium and tellurium scarcity," Prog. Photovolt. Res. Appl. **20**(6), 816–831 (2012).
[103]A. Zappettini *et al.*, "Boron oxide encapsulated vertical Bridgman: A method for preventing crystal-crucible contact in the CdZnTe growth," in *2006 IEEE Nuclear Science Symposium Conference Record, San Diego, CA, 29 October–1 November 2006* (IEEE, 2006).
[104]G. Li *et al.*, "Thermal treatment of detector-grade CdZnTe," J. Cryst. Growth **295**(1), 31–35 (2006).
[105]P. Fochuk *et al.*, "Elimination of Te inclusions in $Cd_{1-x}Zn_xTe$ crystals by short-term thermal annealing," IEEE Trans. Nucl. Sci. **59**(2), 256–263 (2012).
[106]C. Szeles, "Cdznte and CdTe materials for x-ray and gamma ray radiation detector applications," Phys. Status Solidi B **241**(3), 783–790 (2004).
[107]P. J. Sellin *et al.*, "Drift mobility and mobility-lifetime products in CdTe:Cl grown by the travelling heater method," IEEE Trans. Nucl. Sci. **52**(6), 3074–3078 (2005).
[108]O. S. Babalola *et al.*, "Study of Te inclusions in CdMnTe crystals for nuclear detector applications," J. Cryst. Growth **311**(14), 3702–3707 (2009).
[109]K. Kim, J. Hong, and S. Kim, "Electrical properties of semi-insulating $CdTe_{0.9}Se_{0.1}$:Cl crystal and its surface preparation," J. Cryst. Growth **310**(1), 91–95 (2008).
[110]R. Hofstadter, "Thallium halide crystal counter," Phys. Rev. **72**(11), 1120–1121 (1947).
[111]K. S. Shah *et al.*, "Thallium bromide radiation detectors," IEEE Trans. Nucl. Sci. **36**(1), 199–202 (1989).
[112]K. Hitomi *et al.*, "Characterization of thallium bromide crystals for radiation detector applications," J. Cryst. Growth **225**(2–4), 129–133 (2001).
[113]M.-H. Du, "First-principles study of native defects in TlBr: Carrier trapping, compensation, and polarization phenomenon," J. Appl. Phys. **108**(5), 053506 (2010).
[114]K. Hitomi *et al.*, "Polarization phenomena in TlBr detectors," IEEE Trans. Nucl. Sci. **56**(4), 1859–1862 (2009).
[115]K. Hitomi, T. Shoji, and Y. Niizeki, "A method for suppressing polarization phenomena in TlBr detectors," Nucl. Instrum. Methods Phys. Res. A **585**(1–2), 102–104 (2008).
[116]H. Kim *et al.*, "Continued development of thallium bromide and related compounds for gamma-ray spectrometers," Nucl. Instrum. Methods Phys. Res. A **629**(1), 192–196 (2011).
[117]K. Hitomi *et al.*, "TlBr capacitive Frisch grid detectors," IEEE Trans. Nucl. Sci. **60**(2), 1156–1161 (2013).
[118]W. R. Willig, "Mercury iodide as a gamma spectrometer," Nucl. Instrum. Methods **96**(4), 615–616 (1971).
[119]J. E. Baciak and Z. He, "Comparison of 5 and 10 mm thick HgI_2 pixelated γ-ray spectrometers," Nucl. Instrum. Methods Phys. Res. A **505**(1–2), 191–194 (2003).
[120]E. Ariesanti, A. Kargar, and D. S. McGregor, "Mercuric iodide crystal growth and Frisch collar detector fabrication," Nucl. Technol. **175**(1), 124–130 (2011).
[121]J. Peters *et al.*, "Alkali metal chalcogenides for radiation detection," in *MRS Proceedings* (Cambridge University Press, 2011).
[122]J. Im *et al.*, "Formation of native defects in the γ-ray detector material $Cs_2Hg_6S_7$," Appl. Phys. Lett. **101**(20), 202103 (2012).
[123]G. Anandha Babu *et al.*, "Growth improvement of $AgGaSe_2$ single crystal using the vertical Bridgman technique with steady ampoule rotation and its characterization," J. Cryst. Growth **338**(1), 42–46 (2012).
[124]E. Tupitsyn *et al.*, "Lithium containing chalcogenide single crystals for neutron detection," J. Cryst. Growth **393**, 23–27 (2014).
[125]Y. Cui *et al.*, "Defects in $^6LiInSe_2$ neutron detector investigated by photo-induced current transient spectroscopy and photoluminescence," Appl. Phys. Lett. **103**(9), 092104 (2013).
[126]A. C. Stowe *et al.*, "Improving neutron detection in semiconducting $^6LiInSe_2$," Proc. SPIE **9213**, 92130B (2014).
[127]B. Wiggins *et al.*, "Scintillation properties of semiconducting $^6LiInSe_2$ crystals to ionizing radiation," Nucl. Instrum. Methods Phys. Res. A **801**, 73–77 (2015).
[128]B. Wiggins *et al.*, "Investigations of $^6LiIn_{1-x}Ga_xSe_2$ semi-insulating crystals for neutron detection," Proc. SPIE **9593**, 95930B (2015).
[129]N. Singh *et al.*, "Design and growth of novel compounds for radiation sensors: Multinary chalcogenides," Proc. SPIE **9824**, 982411 (2016).
[130]S. S. Kostina *et al.*, "Charge transport mechanisms in a $Pb_2P_2Se_6$ semiconductor," ACS Photonics **3**(10), 1877–1887 (2016).
[131]K. S. Shah *et al.*, "Lead iodide x-ray detection systems," Nucl. Instrum. Methods Phys. Res. A **380**(1), 266–270 (1996).
[132]P. M. Johns, J. E. Baciak, and J. C. Nino, "Enhanced gamma ray sensitivity in bismuth triiodide sensors through volumetric defect control," Appl. Phys. Lett. **109**(9), 092105 (2016).
[133]S. Roth and W. R. Willig, "Lead iodide nuclear particle detectors," Appl. Phys. Lett. **18**(8), 328–330 (1971).
[134]T. Shoji *et al.*, "Fabrication of a nuclear radiation detector using the PbI crystal and its response characteristics for gamma-rays," IEEE Trans. Nucl. Sci. **45**(3), 581–584 (1998).
[135]X. H. Zhu *et al.*, "Growth and characterization of a PbI_2 single crystal used for gamma ray detectors," Cryst. Res. Technol. **42**(5), 456–459 (2007).
[136]V. Deich and M. Roth, "Improved performance lead iodide nuclear radiation detectors," Nucl. Instrum. Methods Phys. Res. A **380**(1), 169–172 (1996).
[137]R. A. Street *et al.*, "Comparison of PbI_2 and HgI_2 for direct detection active matrix x-ray image sensors," J. Appl. Phys. **91**(5), 3345–3355 (2002).
[138]G. Zentai *et al.*, "Large area mercuric iodide and lead iodide x-ray detectors for medical and non-destructive industrial imaging," J. Cryst. Growth **275**(1), e1327–e1331 (2005).

Published under license by AIP Publishing.

[139]K. S. Shah *et al.*, "X-ray imaging with PbI_2-based a-Si:H flat panel detectors," Nucl. Instrum. Methods Phys. Res. A **458**(1–2), 140–147 (2001).
[140]K. Shah *et al.*, "Lead iodide optical detectors for gamma ray spectroscopy," in *1996 Nuclear Science Symposium. Conference Record, Anaheim, CA, 2–9 November 1996* (IEEE, 1996).
[141]K. S. Shah *et al.*, "Characterization of indium iodide detectors for scintillation studies," Nucl. Instrum. Methods Phys. Res. A **380**(1–2), 215–219 (1996).
[142]V. Riabov, *Purification and Crystal Growth of InI and Alloys* IN_{1-x} TL_xI *and* $IN_{1-x}GA_xI$ *for Application in X-Ray and Gamma-Ray Detectors* (Illinois Institute of Technology, 2016).
[143]D. Nason and L. Keller, "The growth and crystallography of bismuth tri-iodide crystals grown by vapor transport," J. Cryst. Growth **156**(3), 221–226 (1995).
[144]Y. N. Dmitriyev *et al.*, "Bismuth iodide crystals as a detector material: Some optical and electrical properties," Proc. SPIE **3768**, 521–529 (1999).
[145]M. Matsumoto *et al.*, "Bismuth tri-iodide crystal for nuclear radiation detectors," IEEE Trans. Nucl. Sci. **49**(5), 2517–2520 (2002).
[146]H. Han *et al.*, "Defect engineering of BiI_3 single crystals: Enhanced electrical and radiation performance for room temperature gamma-ray detection," J. Phys. Chem. C **118**(6), 3244–3250 (2014).
[147]S. S. Gokhale *et al.*, "Fabrication and testing of antimony doped bismuth tri-iodide semiconductor gamma-ray detectors," Radiat. Meas. **91**, 1–8 (2016).
[148]P. M. Johns *et al.*, "Superheating suppresses structural disorder in layered BiI_3 semiconductors grown by the Bridgman method," J. Cryst. Growth **433**, 153–159 (2016).
[149]P. M. Johns, *Materials Development for Nuclear Security: Bismuth Triiodide Room Temperature Semiconductor Detectors* (University of Florida, 2017).
[150]Y. He *et al.*, "High spectral resolution of gamma-rays at room temperature by perovskite $CsPbBr_3$ single crystals," Nat. Commun. **9**(1), 1609 (2018).
[151]D. N. Dirin *et al.*, "Solution-grown $CsPbBr_3$ perovskite single crystals for photon detection," Chem. Mater. **28**, 8470 (2016).
[152]X. Zhao *et al.*, "Nanosecond x-ray detector based on high resistivity ZnO single crystal semiconductor," Appl. Phys. Lett. **108**(17), 171103 (2016).
[153]W. Adam *et al.*, "Review of the development of diamond radiation sensors," Nucl. Instrum. Methods Phys. Res. A **434**(1), 131–145 (1999).
[154]A. Metcalfe *et al.*, "Development of high temperature, radiation hard detectors based on diamond," Nucl. Instrum. Methods Phys. Res. A. **845**, 128 (2017).
[155]T. Williams *et al.*, "Operation of a fast diamond γ-ray detector at the HIγS facility," Nucl. Instrum. Methods Phys. Res. A **830**, 391–396 (2016).
[156]F. Foulon *et al.*, "CVD diamond films for radiation detection," IEEE Trans. Nucl. Sci. **41**(4), 927–932 (1994).
[157]N. G. Wright and A. B. Horsfall, "Sic sensors: A review," J. Phys. D Appl. Phys. **40**(20), 6345 (2007).
[158]G. Bertuccio *et al.*, "Silicon carbide for alpha, beta, ion and soft x-ray high performance detectors," in *Materials Science Forum* (Trans Tech Publications, 2005).
[159]S. Jiang *et al.*, "Balance lead in solution-processed $CH_3NH_3PbBr_xCl_{(3-x)}$ single crystals for high performance x-ray detection," Mater. Lett. **236**, 26–29 (2019).
[160]X. Wang *et al.*, "Ultrafast ionizing radiation detection by p–n junctions made with single crystals of solution-processed perovskite," Adv. Electron. Mater. **4**(11), 1800237 (2018).
[161]L. Carman *et al.*, "Solution-grown rubrene crystals as radiation detecting devices," IEEE Trans. Nucl. Sci., **64**(2), 781 (2017).
[162]S. R. Manohara *et al.*, "On the effective atomic number and electron density: A comprehensive set of formulas for all types of materials and energies above 1 keV," Nucl. Instrum. Methods Phys. Res. B **266**(18), 3906–3912 (2008).
[163]T. Hakamata *et al.*, "The nature of free-carrier transport in organometal halide perovskites," Sci. Rep. **6**, 19599 (2016).
[164]M.-H. Du, K. Biswas, and D. J. Singh, "Resistivity, carrier trapping, and polarization phenomenon in semiconductor radiation detection materials," Proc. SPIE **8507**, 85070M (2012).
[165]*N42.48-2008 American National Standard Performance Requirements for Spectroscopic Personal Radiation Detectors (SPRDs) for Homeland Security* (ANSI, 2008), pp. 1–35.
[166]K. E. Nelson, T. B. Gosnell, and D. A. Knapp, *The Effect of Gamma-Ray Detector Energy Resolution on the Ability to Identify Radioactive Sources* (Lawrence Livermore National Lab, LLNL, Livermore, CA, 2009).
[167]S. E. Anderson, J. Kim, and Z. He, "Event classification in 3d position sensitive semiconductor detectors," in *2008 IEEE Nuclear Science Symposium Conference Record* (IEEE, 2008).
[168]G. A. Armantrout *et al.*, "What can be expected from high-Z semiconductor detectors?," IEEE Trans. Nucl. Sci. **24**(1), 121–125 (1977).
[169]J. Bornstein and R. H. Bube, "Photoelectronic properties of HgI_2," J. Appl. Phys. **61**(7), 2676–2678 (1987).
[170]F. P. Doty *et al.*, "Properties of CdZnTe crystals grown by a high pressure Bridgman method," J. Vacuum Sci. Technol. B **10**(4), 1418–1422 (1992).
[171]J. Franc *et al.*, "Cdte and CdZnTe crystals for room temperature gamma-ray detectors," Nucl. Instrum. Methods Phys. Res. A **434**(1), 146–151 (1999).
[172]C. Szeles, "CdZnTe and CdTe crystals for medical applications," in *Radiation Detectors for Medical Imaging* (CRC Press, 2015), Vol. 45, p. 1.
[173]K. Hitomi, T. Shoji, and K. Ishii, "Advances in TlBr detector development," J. Cryst. Growth **379**, 93–98 (2013).

Published under license by AIP Publishing.